
Methodology For Estimating Helicopter Performance and Weights Using Limited Data

Claudio Baserga, Charles Ingalls, Henry Lee, and Richard Peyran
Aeroflightdynamics Directorate, U. S. Army Aviation Research and Technology Activity,
Ames Research Center, Moffet Field, California

April 1991



National Aeronautics and
Space Administration

Ames Research Center
Moffett Field, California 94035-1000



US ARMY
AVIATION
SYSTEMS COMMAND

AVIATION RESEARCH AND
TECHNOLOGY ACTIVITY
MOFFETT FIELD, CA 94305-1099

NOMENCLATURE

A	rotor disk area, ft ²
B	tip loss factor, N.D.
CDAVG	rotor average profile drag coefficient, N.D.
CD0	rotor average profile drag coefficient (CDAVG) at CLAVG = 0.0, N.D.
C _d	airfoil section drag coefficient
CFNUH	rotor-induced power empirical parameter due to nonuniform inflow in hover, N.D.
CFNUI	rotor-induced power empirical parameter due to nonuniform inflow in forward flight, N.D.
CLAVG	rotor average lift coefficient, N.D.
C _l (1, 90)	airfoil section coefficient of lift at tip of advancing blade, N.D.
CSTL	stall blade-loading equation parameter, N.D.; see equation (9)
C _T	thrust coefficient = THRUST /($\rho A V_{tip}^2$), N.D.
C ₀ , C ₁ , C ₂ , C ₃ , C ₄	coefficients used in drag divergence Mach number equation, N.D.
DCDM	delta main rotor drag coefficient due to compressibility, N.D.
DRSYP	drive system rated power, shp
DSTL	stall blade-loading equation parameter, N.D.; see equation (9)
ESTL	stall power-equation exponent, N.D.; see equation (10)
FK	CDAVG equation empirical parameter, N.D.; see equation (4)
FMU	advance ratio (free-stream velocity divided by rotor tip speed), N.D.
FSTL	stall power-equation empirical parameter, N.D.; see equation (10)
GBLOSS	percent gearbox loss at rated power (DRSYP)
HPCMPR	main rotor compressibility power, shp
HPIND	main rotor induced power, shp
HPPROF	main rotor profile power in forward flight, shp
HPSTAL	main rotor stall power, shp
HPTT	output power required from transmission, shp
HPXMSN	transmission power loss, shp
HPOHOV	main rotor profile power in hover, shp
ISA	international standard atmosphere
KD	engine pressure lapse rate, N.D.; see equation (14)
KT	engine temperature lapse rate, N.D.; see equation (14)
K1	intercept of fuel flow rate vs shp curve, SL/ISA, value normalized by SHP(1,1,0), lb/hr/shp; see equation (15)
K2	slope of fuel flow rate vs shp curve, SL/ISA, lb/hr/shp; see equation (15)
M	Mach number
MCP	maximum continuous power, shp
Mdd	drag divergence Mach number, N.D.
MF	parameter used to adjust K1 for the effects of ambient temperature and pressure changes, N.D.; see equation (15)
N	parameter used to calibrate the ram air effect on SHP available, N.D.; see equation (14)

~~PRECEDING PAGE BLANK NOT FILMED~~

PAGE 11 INTENTIONALLY BLANK

N.D.	nondimensional
NF	parameter used to calibrate the ram air effect on fuel flow, N.D.; see equation (15)
PPFAC	factor for the effect of advance ratio on profile power
SFC	specific fuel consumption, lb/hr-hp
SHP	engine power required, shp
$SHP(\delta, \theta, M)$	engine output power available, shp
$SHP(1, 1, 0)$	engine rated power at sea level/ISA, static conditions (i.e., $\delta = 1$, $\theta = 1$, $M = 0$), shp
SL	sea level
SLS	sea level standard (ISA)
STALPT	blade loading (C_T/σ) at the stall onset point, N.D.
THRUST	rotor thrust, lb
TQU	drive system (output power required)/(rated power), N.D.
VIND	momentum theory induced velocity, ft/sec
V_{tip}	rotor tip speed, ft/sec
WF	fuel flow rate, lb/hr
X	blade-root cutout (fraction of rotor radius), N.D.
XMSN	transmission (drive system)
δ	(ambient pressure, lb/ft ²)/(SLS pressure, ft ²), N.D.
δ_m	ram pressure ratio = $(1 + 0.2 \eta M^2)^{3.5}$, N.D.
η	inlet ram pressure recovery efficiency, N.D.
θ	(ambient temperature, °R)/(SLS temperature, °R), N.D.
θ_m	ram absolute temperature ratio = $(1 + 0.2 M^2)$, N.D.
ρ	ambient air density, slug/ft ³
σ	rotor geometric solidity, N.D.

SUMMARY

A method is developed and described for estimating the flight performance and weights of a helicopter for which limited data are available. The method is based on assumptions that couple knowledge of the technology of the helicopter under study with detailed data from well-documented helicopters judged to be of similar technology. The approach, analysis assumptions, technology modeling, and the use of reference helicopter data are discussed. Application of the method is illustrated with an investigation of the Agusta A129 Mangusta helicopter.

INTRODUCTION

It is often necessary for analysts to estimate the performance and weights of a helicopter for which only limited data are available. Detailed data describing the physical and performance characteristics of the study helicopter could be protected because of proprietary or national security interests. Data could also be unavailable because the study helicopter is still in the conceptual or preliminary design phase.

Analysts must be able to generate the most accurate possible performance and weight estimates from whatever data are available. Failure to do so could compromise a competitive position, or cause resources to be expended unnecessarily. Developing a military helicopter that is overdesigned because of requirements based on the faulty assessment of a threat helicopter requires excessive use of resources. A commercial helicopter that falls short of the performance of a competitor's loses sales. These are simplistic examples, but serve to underscore the potential consequences of not being able to make the most of limited data.

The method described in this paper has been used successfully by the U.S. Army Aviation Research and Technology Activity (ARTA) to accurately analyze existing helicopters. It has also been applied to the analysis and evaluation of conceptual designs.

The technology levels assumed to be embodied in the study helicopter are critical to the analysis. The aerodynamic design of the main rotor, the structural design of the airframe (including materials used), and the performance characteristics of the power plant can all be described in terms of technology levels.

The approach for estimating the flight performance and weights of the study helicopter can be outlined as follows:

1. Assume technology levels for key design features of the study helicopter
2. Select reference helicopters that feature technology levels similar to the study helicopter
3. Develop flight performance and weights models for the reference helicopter based on available data
4. Extract parameters from the reference helicopter models that represent key design-feature technology levels

5. Create study helicopter models using available data and the technology-level parameters found above

6. Estimate flight performance and weights of the study helicopter using the models created

Detailed discussions of the method are presented in the following order: flight performance, propulsion system, and weights. Application of the method is illustrated using the Agusta A129 Mangusta (see appendix).

The authors wish to acknowledge the assistance of John M. Davis and Michael P. Scully of the U.S. Army Aviation Research and Technology Activity in the preparation of this report, as well as Cynthia Callahan of the McDonnell Douglas Helicopter Company for her help in developing the CAMRAD model of the AH64.

FLIGHT PERFORMANCE ESTIMATION

Flight performance depends on many critical areas of the study helicopter system (e.g., main- and tail rotor aerodynamic characteristics, airframe lift and drag, propulsion system performance, operating gross weight). The following topics are covered in this section:

1. Performance codes used in the analysis
2. Overview of the modeling approach
3. Method for determining empirical parameters that represent the main rotor aerodynamic technology level
4. Modeling of the tail rotor
5. Method for estimating airframe aerodynamic lift, drag, and moment characteristics

Performance Codes

Two codes are used to estimate the study helicopter flight performance, the ARTA Maneuver Performance Program (MPP), and the Comprehensive Analytical Model of Rotorcraft Aerodynamics and Dynamics (CAMRAD) (refs. 1–3). MPP is a preliminary/conceptual design-level performance code used to model the flight performance of the study helicopter. CAMRAD is a very detailed analysis code used to calibrate MPP to the appropriate main rotor aerodynamic technology level.

MPP is a FORTRAN computer program which models helicopter maneuvering flight performance. MPP uses data that are typically available during the late conceptual or early preliminary design phases of a helicopter development program. Major features of MPP include the following:

1. A quasi-static flight performance calculation for a helicopter throughout its flight envelope

2. An energy method rotor model for power required
3. An airframe aerodynamic model (lift, drag, download, pitching moment)
4. A propulsion system model (power available, fuel flow, net jet thrust)
5. A longitudinal force and moment trim for each flight condition

The quasi-static flight performance calculated by MPP represents the capability (generally, the maximum capability based on engine power or aerodynamic loads) of the helicopter at a given flight condition and does not address the time or flight path required to achieve that flight condition.

The simple energy method model for main rotor power in MPP has several empirical parameters to account for the effects of nonuniform inflow over the rotor disk, rotor-blade twist and planform, and airfoil section lift and drag characteristics for both incompressible and compressible flow. The values used for these empirical parameters represent the main rotor aerodynamic technology level.

The more detailed analysis code, CAMRAD, is used to determine the MPP main rotor empirical parameters. CAMRAD is a blade-element analysis designed to calculate rotor performance, aerodynamic and structural loads, helicopter vibration and gust response, flight dynamics and handling qualities, and aeroelastic stability. CAMRAD calculates the effects of nonuniform inflow over the rotor disk, rotor-blade twist and planform, and airfoil section lift and drag characteristics for both incompressible and compressible flow.

Modeling Approach

The first step in estimating the flight performance of the study helicopter, when using MPP, is to pick a reference helicopter (one for which flight-test data are available) that is thought to incorporate a similar main rotor aerodynamic technology level and to be of similar configuration. The following modeling approach is then used:

1. Develop MPP and CAMRAD input data sets for the reference helicopter
2. Adjust CAMRAD modeling options to achieve the best correlation of CAMRAD with available flight-test data
3. Adjust MPP main rotor empirical parameters for the reference helicopter to achieve the best correlation of the MPP model with available flight-test data and with CAMRAD
4. Validate the MPP data set in flight regimes for which flight-test data are not available by using the calibrated CAMRAD data set
5. Determine the airframe lift, drag, and moment characteristics of the study helicopter; this may use normalized reference helicopter airframe aerodynamic data

6. Determine the propulsion system characteristics of the study helicopter; this may use reference helicopter engine installation and transmission losses
7. Determine the study helicopter operating gross weights
8. Assume that the MPP main rotor empirical parameters developed for the reference helicopter are valid for the study helicopter (based on similar technology levels)
9. Estimate the performance of the study helicopter based on available dimensional data and the determined empirical parameters, airframe aerodynamic characteristics, propulsion system characteristics, and operating gross weights

The described modeling approach is presented in flowchart form (fig. 1). The purpose of correlation with reference helicopter flight-test data is to create and substantiate a reference helicopter model for both the CAMRAD and MPP programs from which the study helicopter model can be developed.

MAIN ROTOR AERODYNAMIC TECHNOLOGY

In MPP, main rotor power required by the helicopter is broken down into the following components: induced, profile, stall, compressibility, and parasite power. The MPP expressions for these power components feature the following empirical parameters (which represent the main rotor aerodynamic technology level):

1. Induced power: empirical parameters for the effects of nonuniform inflow in hover (CFNUH) and in forward flight (CFNUI)
2. Profile power: empirical parameters determine the rotor average profile drag coefficient (CDAVG)
3. Stall power: empirical parameters establish rotor-blade loading (C_T/σ) at the stall onset point (CSTL, DSTL) and the power required (ESTL, FSTL)
4. Compressibility power: empirical parameters determine the drag divergence Mach number (Mdd)
5. Parasite power: empirical parameters used represent airframe aerodynamics (not rotor aerodynamics)

Empirical Parameters

Nonuniform Inflow Parameter Applied to Induced Power

The following equation is used by MPP to calculate the main rotor hover induced power:

$$HPIND = CFNUH | THRUST | VIND/550 \quad (1)$$

The nonuniform inflow parameter applied to the induced power in hover is found by using flight-test data for the reference helicopter in hover. The main rotor power required at hover is determined

from flight-test data and compared with the power calculated by CAMRAD with uniform inflow. The CAMRAD inputs affecting the inflow are adjusted to obtain the best possible correlation with the flight-test data. The induced-power component from CAMRAD is then compared with that calculated using equation (1) (with CFNUH set to 1.0). The MPP hover empirical parameter (CFNUH) is determined from the following:

$$CFNUH = (\text{CAMRAD induced power})/(\text{MPP induced power}) \quad (2)$$

The nonuniform inflow parameter for MPP in forward flight is assumed equal to the hover value for preliminary estimates ($CFNUI = CFNUH$).

Rotor Average Profile Drag Coefficient Applied to Profile Power

The energy-method model used in MPP calculates profile power based on the assumption of a rotor average profile drag coefficient (CDAVG) that is constant over the entire rotor disk. This CDAVG is a function of rotor average lift coefficient (CLAVG). The CDAVG versus CLAVG function used in MPP is calibrated with CAMRAD calculations for the hover case.

MPP calculates main rotor hover profile power from the following equation:

$$HP0HOV = 0.125 \text{ CDAVG}(\sigma \rho AV_{tip}^3)/550 \quad (3)$$

The MPP model for CDAVG used in this analysis is the same one used in recent LHX studies:

$$\text{CDAVG} = CD0 + FK | \text{CLAVG} |^{2.7} \quad (4)$$

To determine the values for the empirical parameters $CD0$ and FK , CAMRAD is used to model the isolated rotor of the reference helicopter in hover at blade loadings (C_T/σ) of 0.02, 0.04, 0.06, 0.07, 0.08, 0.09, 0.10, 0.11, and 0.12. The CDAVG for each condition based on the profile power predicted by CAMRAD is

$$\text{CDAVG} = 4400 \text{ HPPROF}/(\sigma \rho AV_{tip}^3) \quad (5)$$

CLAVG is then calculated from the prescribed values of C_T/σ using the following equation from MPP:

$$\text{CLAVG} = 6(C_T/\sigma)/(B^3 - X^3) \quad (6)$$

A least-squares-error curve fit is applied to the CAMRAD values of CDAVG and the $|\text{CLAVG}|^{2.7}$ to determine the empirical parameters $CD0$ and FK (fig. 2).

The profile power required during forward flight is found from the following equation:

$$\text{HPPROF} = (\text{HP0HOV})(\text{PPFAC}) \quad (7)$$

where (from ref. 4)

$$\text{PPFAC} = 1.0 + (4.5 \text{ FMU}^2) + (1.61 \text{ FMU}^{3.7}) \quad (8)$$

Equation (8) is reasonably accurate for advance ratios (FMU) up to 0.5.

Empirical Parameters Applied to Stall Power

The stall power calculation in MPP is based on C_T/σ . C_T/σ and the stall onset point are calculated at every airspeed and compared. As C_T/σ surpasses the stall onset point, stall effects are calculated. The value of C_T/σ at the stall onset point is calculated by the following equation:

$$\text{STALPT} = \text{CSTL} + \text{DSTL}/(1.0 + 50.0 \text{ FMU}^2)^{0.5} \quad (9)$$

The magnitude of the power required because of stall is calculated from the following equation:

$$\text{HPSTAL} = 0.125(\sigma \rho A V_{\text{tip}}^3 \text{FSTL})(C_T/\sigma - \text{STALPT})^{\text{ESTL}}/550 \quad (10)$$

Values for the empirical parameters CSTL, DSTL, ESTL, and FSTL have been determined from past ARTA studies. These baseline values are used when correlation with flight-test data first begins. An iterative process is used to determine new values for these empirical parameters that improve the correlation of the MPP estimate with the flight-test data.

Drag Divergence Mach Number Applied to Compressibility Power

In determining compressibility power, MPP calculates the airfoil drag divergence Mach number (Mdd). Mdd is defined as the Mach number at which the change in section drag coefficient (C_d) with respect to the change in Mach number equals 0.10 ($\Delta C_d/\Delta M = 0.10$). It is modeled by an equation of the following form:

$$\text{Mdd} = C_0 + C_1 C_l(1, 90) + C_2 C_l(1, 90)^2 + C_3 C_l(1, 90)^3 + C_4 C_l(1, 90)^4 \quad (11)$$

The lift coefficient at the tip of the advancing blade, $C_l(1,90)$, is a function of blade collective pitch, blade twist, the uniform inflow angle, and airfoil aerodynamic characteristics at the tip.

The compressibility effects that occur on the advancing side of the rotor disk take place primarily in the tip region. However, they also occur farther inboard as the local lift requirements cause portions of the blade to operate close to or beyond the drag divergence boundary (ref. 5). For that reason, the equation for Mdd is based on the two-dimensional airfoil characteristics found on the outboard 15% of the reference helicopter rotor blade.

Plots of Mach number versus C_d , for an angle of attack range of -4° to $+4^\circ$, are produced for each airfoil section on the outboard 15% of the rotor. Mdd is located at the point where $\Delta C_d/\Delta M = 0.10$ for each angle of attack. Using the Mdd determined for the particular airfoil and angle of attack, a corresponding section lift coefficient (C_l) is interpolated from the two-dimensional airfoil table. A least-squares-error curve fit of Mdd versus C_l is then produced for each airfoil found on the outboard 15%. The equation of Mdd versus C_l , used in MPP, is an average of the least-squares-error curve fit found for each airfoil.

Once Mdd is calculated, the delta Mach number (ΔM) is found; it is the difference between the advancing-tip Mach number ($M(1,90)$) and Mdd. The delta Mach number is used to determine the increase in main rotor drag caused by compressibility effects as shown below:

$$\text{DCDM} = 0.056(\Delta M) + 0.416(\Delta M)^2 \quad (12)$$

This equation (from ref. 4) is based on reference 6. At low airspeeds, and particularly in hover, this model predicts excessive compressibility power using the MPP Mdd equation. To account for hover and low airspeed it was determined empirically that by artificially fixing the Mdd for $C_l(1,90)$ greater than 0.40, acceptable correlation of MPP with test data can be obtained. The artificial value for Mdd is dependent on the drag characteristics of the airfoils under study. Combined airfoils, which demonstrate a higher Mdd versus C_l curve, will have a higher artificial value of Mdd at $C_l(1,90)$ equal to 0.40.

The compressibility power is then determined from the following equation:

$$\text{HPCMPR} = 0.125 \text{ DCDM}(\sigma \rho A V_{tip}^3) / 550 \quad (13)$$

A flowchart of the method described is presented for a rotor blade with two airfoils located on the outboard 15% (fig. 3).

Tail Rotor Model

As was the case with the MPP main rotor model, the MPP tail rotor model also contains empirical parameters that effect the aerodynamic technology level. These empirical parameters are applied to the induced-, profile-, and stall-power components. The forms of the equations used for the tail rotor are similar to those found for the main rotor. The empirical parameters determined for the main rotor can be applied to the tail rotor. This assumes an equal aerodynamic technology level between the main and tail rotors which is acceptable for initial performance estimates.

Airframe Aerodynamics

Modeling the airframe aerodynamics of the study helicopter can be approached in several ways. A direct approach would be to use wind tunnel test data for the study helicopter airframe (if such test data are available). These data serve as a basis for determining the MPP inputs that model the airframe aerodynamic lift, drag, and moment characteristics.

If wind tunnel data are not available for the study helicopter airframe, the following modeling approach can be used:

1. Select a reference helicopter (for which airframe wind tunnel data are available) whose configuration is similar to that of the study helicopter.
2. Using the wind tunnel test data for the reference helicopter, determine normalized lift, drag, and moment characteristics.
3. Scale the normalized reference helicopter airframe characteristics by the appropriate study helicopter area or volume to estimate the study helicopter airframe characteristics.

Where lift or drag characteristics are not available from wind tunnel tests, textbook methods can be used to estimate the airframe lift, drag, and moment characteristics of the study helicopter.

PROPULSION SYSTEM MODELING

Propulsion system modeling in ARTA's Maneuver Performance Program is divided into four major areas:

1. Uninstalled turboshaft engine performance relationships, which model shaft horsepower (shp) and fuel flow versus ambient temperature, pressure, and velocity
2. Engine-installation effects which account for inlet ram efficiency and losses due to the inlet particle separator (IPS), inlet duct, and infrared suppressor (IRS)
3. Accessory and transmission power losses
4. Engine net jet thrust and the momentum drag associated with operation of the IR suppressor

The modeling approaches used for calculating uninstalled engine performance, fuel consumption, engine-installation effects, and accessory and transmission power losses are presented below. Modeling of engine net jet thrust and IRS momentum drag will not be presented in this paper.

Power Required and Power Available

The power required by the helicopter must be less than or equal to the power available at the engine output shaft for steady-state flight. Power required is defined as the power measured at the engine output shaft during flight. It includes main rotor power, tail rotor power, accessory equipment power, and power loss through the transmission.

Power available is the installed engine power available at the engine output shaft. It is equal to uninstalled engine power plus ram-air effects reduced by the installation losses associated with both inlet and exhaust systems (e.g., IPS, IRS). The components of power available and power required are presented graphically (fig. 4).

Uninstalled Engine Performance Relationships

Based on data from a number of existing engines, the SHP available at any given condition of temperature, pressure, and Mach number can be approximated by the following lapse-rate equation:

$$\text{SHP}(\delta, \theta, M) = \text{SHP}(1, 1, 0)[1 - KT(\theta - 1)][1 + KD(\delta - 1)][\delta_m \sqrt{\theta_m}]^N \quad (14)$$

Calculation of Lapse Rates

Engine power available at a given altitude and temperature is dependent on the engine lapse rates. The lapse rates consist of the temperature lapse rate KT (which measures the effect of ambient temperature changes) and the pressure lapse rate KD (which measures the effect of density changes resulting from pressure altitude changes). For typical gas turbine engines, KT is calculated from engine rated power available at sea level (SL)/ISA and at a SL hot day condition, such as SL/ISA + 20°C.

Pressure lapse rate (KD) is calculated from engine power available (which has been normalized by $1 - KT(\theta - 1)$) versus pressure altitude data. The normalization of power available removes the effects of temperature variations with altitude, so that KD only represents density effects. Thus, all temperature effects are represented by KT. Typically, it requires several KD values to define the entire altitude range. Each KD defines a portion of the altitude range, using a piecewise linear approximation. For example, three KD values (KD1, KD2, KD3) can be used to define an altitude range from sea level ($\delta = 1.0$) to 20,000 feet ($\delta = 0.459$) (fig. 5).

Fuel Flow

Studies of turboshaft engine fuel flow indicate that the fuel-flow rate can be approximated by a linear function of SHP. Typically, the intercept varies with altitude. By curve-fitting the data from a number of existing engines, the following expression was found to represent turboshaft engine fuel-flow rate as a function of temperature, pressure, and Mach number:

$$WF = K1[(\delta\sqrt{\theta})^{MF}]SHP(1, 1, 0) + K2(SHP)/[\delta_m\sqrt{\theta_m}]^{NF} \quad (15)$$

Typically, the intercept (K1) and slope (K2) are calculated by a linear curve fit of engine fuel-flow rate versus horsepower data at SL/ISA. The value for K1 is the intercept fuel-flow value divided by the engine rated power at sea level. The parameter MF calibrates K1 to the effects of variations in ambient temperature and pressure that result from changes in altitude. NF calibrates K2 to the ram-air effect. Values for MF and NF are typically determined for a limited range of operating conditions to best match the fuel-flow data available.

Engine-Installation Effects

Engine-installation effects consist of ram pressure recovery efficiency and inlet duct, IPS, and IRS installation losses. These effects vary depending on details of the particular installation.

Accessory Power Requirements

Study helicopter accessory power includes electrical, hydraulic, and pneumatic requirements. These are estimated based on a reference helicopter with analogous mission requirements. Typically, the same ratio of accessory power to installed power is maintained between the study helicopter and the reference helicopter.

Transmission Power Loss

Modeling of the transmission power loss is based on test results of drive-system efficiency expressed as a linear function of input torque and engine speed. The following modeling equations for transmission power loss (HPXMSN) were developed:

$$HPXMSN = 0.01 \text{ GBLOSS}(2.33 - 1.33TQU)HPTT \quad (\text{if } TQU \geq 0.25) \quad (16)$$

$$HPXMSN = 0.005(\text{GBLOSS})(\text{DRSYP}) \quad (\text{if } TQU < 0.25) \quad (17)$$

WEIGHT ESTIMATION

This section discusses a method for estimating helicopter weight using limited data. The type of helicopter gross weight used as the basis for performance prediction is defined. The gross weight is divided into empty weight and useful load. Useful load items and their weights are identified. Empty weight is decomposed into group weights of sufficient detail for estimation. The groups are categorized as either "scaled" or "fixed." Assumptions are made concerning areas of uncertainty. Scaled weights are estimated using calibrated parametric relationships. Fixed weights are estimated using analogous weights from reference helicopters. Weight estimates are verified and combined to arrive at the helicopter weight estimate.

Helicopter Weight Groups

Gross weight is defined in reference 7 as "the weight of a vehicle, fully equipped and serviced for operation..." There are several kinds of gross weight. Maximum takeoff gross weight (VTOL aircraft) commonly expresses the maximum weight at which a vertical takeoff can be achieved. It is one of the most frequently cited weights in published literature. Primary-mission gross weight is the weight of the helicopter configured with the fuel, weapons, crew, and equipment required to perform its primary mission. It is particularly relevant to predicting the performance of a helicopter in its intended role (typically the mission for which the design is optimized). The type of gross weight to be used for analysis is identified in order to define the study helicopter configuration and useful load.

Gross weight can be decomposed into empty weight and useful load. Empty weight describes the helicopter weight without useful load, and is discussed in more detail below. Useful load includes the weights of crew, fuel and fluids (usable and trapped), internally carried expendables (e.g., ammunition), and stores. It also includes other removable items that are not essential to helicopter operation.

Empty weight is composed of four functional weight groups: structure, propulsion, flight control, and equipment. The functional weight groups are decomposed further, into weight groups based on Part I (Group Weight Statement) of Military Standard 1374A (ref. 8). The functional group Structure, for example, includes the weights of wing, main rotor, tail, and other weights related to airframe structures.

As more detail is required, the Part I weight groups are subdivided into components, and collections of components, based on Part II (Detail Weight Statement) of reference 8. For example: the weight group Main Rotor can be subdivided into blades, and hub and hinge. Decomposition of gross weight into components is illustrated graphically in figure 6.

Helicopter gross weight is systematically resolved, using the preceding approach, from gross weight to the level of detail required for accurate estimation. The level of detail required depends on the accuracy of estimation needed, the accuracy and precision of the estimation tools applied, and the information available.

Helicopter Weight Estimation Categories

Weight groups, after decomposition to the appropriate level of detail for estimation, are categorized either as scaled (dependent on helicopter characteristics) or fixed (dependent on mission requirements). Categories of groups are determined by the weight relationships that drive their weights. The weight relationships determine the methods used for weight estimation.

Scaled Weights

Scaled weights are those dependent on physical quantities that describe helicopter size and configuration characteristics (such as length, area, volume, number of rotor blades). Rotors, fuselage, and landing gear are examples of scaled weight groups. Estimation methods include statistical and nonstatistical parametric equations. Scaled weight components are assumed to incorporate specific levels of technology and military requirements. Military requirements include vulnerability reduction (e.g., ballistically tolerant components), crashworthiness enhancements (e.g., energy absorbing fuselage structures and breakaway fuel system fittings), and susceptibility reduction (e.g., flat-plate canopies and infrared suppression).

Fixed Weights

Fixed weights are those that depend on mission requirements instead of on physical quantities. Mission requirements include military requirements, which also influence scaled weights, and functional requirements. Military requirements affect fixed weight groups that contribute to crashworthiness (e.g., stroking crewseats in furnishings and equipment), ballistic tolerance (e.g., parasitic armor in armament), and nuclear, biological, and chemical (NBC) protection (e.g., NBC filters in air conditioning). Fixed weight components include communication, target acquisition and identification, navigation, fire control, aircraft survivability equipment (ASE), anti-icing and armament installation, and are directly influenced by functional requirements (e.g., the need to acquire and identify targets at night).

Helicopter Weight Estimation Methods

The mission gross weight is the sum of empty weight and mission useful load. The intended helicopter mission will define useful load items: weapons load to be carried, fuel necessary to accomplish the primary mission, additional fuel required for reserve and contingency planning, and crewmembers with their equipment. The weights of weapons and associated provisions are listed in various publications. Fuel and crew weights are calculated using published information (e.g., weight of 95th percentile Army aviator, from ref. 9).

Scaled Weight Estimation

Levels of military requirements and technology must be assumed before weight estimation if they do not appear in available information sources. Military requirement assumptions address issues such as levels of ballistic tolerance and crashworthiness designed into the airframe. Technology assumptions specify how component weights vary with respect to those of the reference helicopter.

Parameters (helicopter characteristics) that drive group weights are identified. Parameters that significantly affect weight (independent variables) are found for each group to be estimated (dependent variable). Data (parameter values and group weights) to be used for defining the relationships between the parameters and the group weights are selected. Sources of data are identified and collection commences. Parametric weight equations are generated statistically, or by other means, using the data collected.

The weight equations generated in the preceding step are calibrated against the reference helicopter so that they can more accurately represent the study helicopter. Group weights are estimated using the reference helicopter parameter values. The estimated weights are compared with the actual weights of the reference helicopter and then the calibration factors that cause them to be equal are determined. Factors that reflect the weight effect of advanced technologies (e.g., composite materials) and military requirements are also determined. An example is demonstrated for the AH-64 main rotor (fig. 7).

Scaled weights are estimated using parametric weight equations with the study helicopter input parameters. Calibration factors are applied to estimates, along with any applicable factors to account for advanced technology and military requirements.

Fixed Weight Estimation

Fixed weights are estimated differently than scaled weights, but similar assumptions are required. Fixed weight assumptions, like those for scaled weights, address the study helicopter levels of military requirements and technology. Assumptions are also made regarding similarities of the study helicopter functional requirements (based on mission and capabilities) to those of the reference helicopter.

The mission requirements that drive fixed weights are defined by the assumed mission and capabilities of the study helicopter. A reference helicopter with similar missions and capabilities is identified. Fixed weight groups of the study helicopter are assumed to be equal to the functionally analogous weight groups of the reference helicopter. Group weights estimated in this way can be adjusted for the effect of advanced technologies by applying technology factors.

Helicopter Weight Estimation Verification

The study helicopter weight estimates are checked to ensure that they are reasonable. A number of checks are available. One is to compare scaled weights with data used to generate the original parametric weight equations. The parameter values for the study helicopter are compared with the parameter values of other helicopters, and differences are evaluated. Fixed weights of the study helicopter are also compared with those of other helicopters. Gross weight fractions are used to check both scaled and fixed weights. The study helicopter weights, and the weights of other helicopters, are reduced to a fraction of the gross weight and their contributions compared.

CONCLUDING REMARKS

A method has been presented for estimating the flight performance and weights of helicopters using limited available data. The method is based on assumptions regarding the technology levels embodied in the study helicopter and on assumed similarities with reference helicopters.

The method is demonstrated using the Agusta A129 Mangusta as an example (AH-1 Cobra and AH-64 Apache serve as reference helicopters). Estimated A129 flight performance values are found to compare well with published values. Maximum speed and maximum rates of climb are estimated within 3% of published values. The estimated vertical rate of climb is 40% higher than the published value (at 4000 ft/ISA). This can be explained by a low ARTA estimate for vertical flat-plate drag. The estimated A129 weights and weight fractions are found to compare well with published values. The A129 estimated empty weight is 1.8% greater than the published value. Estimated A129 scaled weight fractions are within 2% of comparable AH-64 weight fractions. There are larger differences in fixed weight fractions, but these are attributable to differences in A129 and AH-64 mission requirements.

Reasonably accurate estimates of flight performance and weights can be generated using the method presented. The estimates can be easily revised as new information on the study helicopter becomes available. In addition, sensitivity studies can be performed to address the uncertainty in the assumed technology levels for the study helicopter. These sensitivity studies result in a performance band, where the upper limit of performance represents the most advanced technology levels that can reasonably be assumed.

APPENDIX

FLIGHT PERFORMANCE AND WEIGHTS ESTIMATION EXAMPLE

The flight performance and weights of the Agusta A129 Mangusta were estimated using the method described in this report. The estimates were made using available published data. In areas for which data were not available, assumptions were made based on similarities in levels of technology between the A129 helicopter and reference helicopters.

A129 DESCRIPTION

The A129 was designed as a light combat helicopter for Italian Army use, primarily in the anti-tank role. It features a 39.04-ft diameter, articulated main rotor system with four composite blades and a 7.35-ft diameter, semirigid tail rotor system with two composite blades. The crew is seated in tandem with the pilot seated aft of and above the weapons operator. The mid-fuselage mounted composite wing has four pylons for mounting stores. Propulsion is provided by twin pod-mounted Rolls-Royce Gem 2 Mk 1004D engines (henceforth referred to as Gem 2). Each engine has a sea level standard (SLS) intermediate rated power (IRP) of 881 shp. The landing gear is a nonretractable tailwheel type (refs. 10-12). The three-view drawing in figure 8 illustrates the A129 configuration.

The A129 is similar in configuration and intended mission to the AH-64. The following are features common to both the A129 and the AH-64:

1. Articulated main rotor system, four composite blades
2. Twin, pod-mounted, front-drive engines
3. Crashworthy, nonretracting, tailwheel-type landing gear
4. Tandem crew stations
5. Mid-fuselage mounted wing with external stores stations
6. Survivability and crashworthiness enhancement features

Though very similar to the AH-64 in configuration, in terms of physical size and weight the A129 is closer to the AH-1. The following are features common to both the A129 and the AH-1:

1. Two-blade tail rotor mounted high on the vertical tail
2. Mid-fuselage mounted wing with external stores stations
3. Tandem crew stations
4. Small horizontal stabilizer mounted on tail boom

Side views of the A129, the AH-64, and the AH-1 are presented for comparison in figure 9.

A129 MODELING DATA AND ANALYSIS ASSUMPTIONS

Available published data were used to determine many of the characteristics of the A129, including dimensions, mission equipment, military requirements, limited engine performance data, and gross weights. Specific available data used to model flight performance, propulsion system performance, and weights are presented in tables cited throughout this appendix.

Several assumptions, combined with detailed data from well-documented reference helicopters were used to determine characteristics for which A129 data were unavailable. The AH-64 and the AH-1 served as reference helicopters for modeling the A129 flight performance and weights. The T700-GE-701 and Advanced Technology Demonstrator Engines (ATDE) served as reference engines for modeling the Gem 2.

The following list summarizes the assumptions made in analyzing the A129:

1. Main rotor aerodynamic technology level equal to AH-64
2. Airframe aerodynamics represented by AH-64 scale-model wind tunnel test data
3. Gem 2 lapse rates equal to the average of T700-GE-701 and ATDE
4. Gem 2 ram-air effect parameters equal to ATDE
5. Engine-installation losses as a percentage of rated power equal to AH-64
6. AH-64 or AH-1 levels of military requirements and technology for scaled weights
7. AH-64 levels of military and functional requirements for fixed weights

A129 FLIGHT PERFORMANCE ESTIMATION

To estimate the flight performance of the A129, the main rotor aerodynamic technology level for the AH-64 had to first be determined. The aerodynamic technology level in the MPP analysis is established by the values used for the rotor empirical parameters.

The physical characteristics of the AH-64 (radius, tip speed, wing area, etc.) were available from McDonnell Douglas Helicopter Co. (MDHC) scale drawings, weight reports, and the Air Vehicle Technical Description (ADS-10) document (refs. 13 and 14). The aerodynamic characteristics of the AH-64 fuselage, horizontal tail, and wing were obtained from a NASA/Army wind tunnel test (ref. 15). Using the available information, and data provided by MDHC, an AH-64 CAMRAD deck was created. Since CAMRAD does not calculate total rotorcraft flight performance, it was necessary to determine transmission and accessory losses for each flight condition tested. These losses were estimated using the expressions discussed in the Propulsion System Modeling section in the main text. The total CAMRAD predicted power and the calculated transmission and accessory powers were added. This total power

required was correlated with flight-test results. The AH-64 flight-test conditions and the specific losses applied to the CAMRAD results are presented in tables 1 and 2.

Upon satisfactory correlation between CAMRAD and flight test, an MPP input deck for the AH-64 was created. The same physical characteristics and airframe aerodynamic data were used. To correlate with CAMRAD and flight-test results, it was necessary to determine the MPP empirical parameters which represent the main rotor aerodynamic technology level for the AH-64. The determination of these empirical parameters follows in more detail.

AH-64 Main Rotor Aerodynamic Technology Level

The AH-64 flight-test data and the correlated CAMRAD results were used to establish the AH-64 empirical parameters which represent the main rotor aerodynamic technology level. The nonuniform inflow coefficient (CFNUH, CFNUI), the rotor average profile drag coefficient (CDAVG), the stall coefficients (CSTL, DSTL, *ESTL*, FSTL), and the drag divergence Mach number (Mdd) equation were determined for the AH-64 using the method presented previously. A brief discussion is presented below for each of these empirical parameters. The specific values determined for these empirical parameters are presented in table 3.

Coefficient of Nonuniform Inflow (CFNUH)

AH-64 hover nondimensional flight performance data (ref. 16) and the hover CAMRAD results (uniform wake) were used to determine CFNUH. Upon achieving satisfactory correlation between CAMRAD and flight test, the CAMRAD induced power was compared with that predicted by MPP. By using equation (2), CFNUH was determined for use in MPP. This value of CFNUH was also used in forward flight for CFNUI.

Rotor Average Profile Drag Coefficient (CDAVG)

CAMRAD was used to model an isolated AH-64 rotor in hover at various blade loadings (C_T/σ) to determine CDAVG. CAMRAD calculates the CDAVG for each condition based on the predicted profile power. From the C_T/σ , the root cutout, and an assumed tip-loss factor, the rotor average lift coefficient (CLAVG) was calculated (see eq. (6)). Using a least-squares-error curve fit of the CAMRAD CDAVG versus $|\text{CLAVG}|^{2.7}$, the values for the empirical parameters CD0 and FK were determined (fig. 10).

Notice that the CAMRAD raw data points plotted in figure 10 show some scatter from the fitted curve. To help assess the importance of the scatter, the profile power was calculated for both the raw data point and the corresponding fitted curve at several C_T/σ . Results indicated that the horsepower difference between the raw data points and the least-squares-error curve fit was small, verifying that the curve fit used was sufficiently accurate.

Stall Coefficients (CSTL, DSTL, ESTL, FSTL)

The values of the empirical parameters that represent the stall effects for the AH-64 were determined through an iterative process. The analysis began with baseline values for these empirical parameters

which were derived from past ARTA studies. Calibration with both flight-test data and CAMRAD main rotor power required led to the final values used.

Drag Divergence Mach Number (Mdd)

The main rotor airfoils present on the outboard 15% radius of the AH-64 are the HH02 and the NACA 64A006. As presented in figure 3, the Mdd was determined for each airfoil. This was accomplished based on the individual two-dimensional lift and drag characteristics for each airfoil. Plots were produced of Mach number versus the coefficient of drag (C_d) for a range of angles of attack. Mdd was located at the approximate point at which $\Delta C_d / \Delta M = 0.10$ for a given angle of attack. The lift coefficient (C_l) for each Mdd was interpolated from the airfoil table and then plotted against Mdd. A least-squares-error curve fit of the data was used for each airfoil. The equation of Mdd versus C_l (see eq. (11)), used in MPP, is a mean least-squares-error curve fit of the data from both airfoils (fig. 11).

As stated in the methodology description, when the derived Mdd equation was applied, it was found to overpredict compressibility power at hover and low airspeeds. To remedy this situation it was necessary to artificially set the Mdd for C_l greater than 0.4 (fig. 12).

AH-64 MPP Performance Estimate

The AH-64 estimated performance using MPP, with the derived main rotor empirical parameters, was compared with flight-test data (ref. 17) and CAMRAD results (figs. 13-15). It is evident from the flight-test conditions available, that the correlation of MPP and CAMRAD with flight-test data was limited to high pressure-altitudes and high temperatures (see table 1). Therefore, predicting performance for the AH-64 at ISA conditions involves an extrapolation of methods and results. This limitation is unavoidable because AH-64 flight-test data at conditions other than those in the AEFA report are not available. To mitigate this limitation, the validated CAMRAD data set was run for SLS conditions and compared with MPP results at SLS. The rationale for doing so is as follows: CAMRAD is a blade-element model which uses two-dimensional airfoil data to calculate stall and compressibility effects. This approach is much closer to an experimental data base (two-dimensional airfoil wind tunnel tests) than the empirical stall and compressibility models in MPP. Hence, if CAMRAD is well correlated with a set of test data that corresponds to a relatively broad range of atmospheric conditions, it is reasonable to assume that CAMRAD can be used to extrapolate outside this range. Correlation between CAMRAD and MPP at SLS conditions was good, which indicates that the MPP compressibility model could be extrapolated to SLS conditions (fig. 16).

A129 MPP Input Data

The correlated MPP AH-64 input data set was used as a base for the A129 flight performance estimate. The A129 physical characteristics (e.g., rotor radius, solidity, tip speed, gross weight, wing area, empennage area) were obtained from available literature. These values were substituted for the base input values of the AH-64. MPP input data concerning the fuselage lift characteristics were determined for the A129 by normalizing the AH-64 input values with the AH-64 area or volume and then multiplying this normalized value by the appropriate estimate of A129 area or volume. The MPP input parameters that describe the AH-64 wing and empennage lift characteristics are already normalized

to area and could be used directly for the A129. The A129 drag characteristics were estimated based on methods found in Hoerner (ref. 18) by using A129 specific dimensions. Finally, the main rotor empirical parameters determined for the AH-64 were used directly for the A129 implying equal levels of aerodynamic technology between the helicopters.

A flowchart of the method involved in determining the A129 input data set and flight performance is shown in figure 17. Input values used for the A129 analysis are tabulated in tables 4-9.

A129 PROPULSION SYSTEM MODEL

The A129 is powered by two Rolls-Royce Gem 2 turboshaft engines mounted side by side, aft of the main rotor gearbox. The engine has an integral inlet particle separator (IPS). The installation in the A129 includes a dynamic air intake system and an infrared suppressor (IRS) system. The methods used for modeling the uninstalled engine performance and the installation losses are presented below.

Gem 2 Power Available and Fuel Flow Data

A summary of the Gem 2 engine performance is presented in table 10. These are typical data that are publicly available for turboshaft engine performance and are only for sea level standard (SLS) conditions with the engine operating statically. Additional engine performance data at other operating conditions are required to develop a complete engine model for a full range of operating conditions. Since these data were not publicly available, assumptions were made based on characteristics of two reference engines, the ATDE and the T700-GE-701.

Comparisons with ATDE and T700-GE-701

The ATDE is close to the Gem 2 in terms of rated shaft horsepower and output rpm, but represents early 1980s engine technology (Gem 2 is mid-1970s technology). Compared with the Gem 2, the T700-GE-701 has a larger rated shaft horsepower, a lower output rpm, and a higher pressure ratio (both engines represent 1970s technology). A comparison of the Gem 2 with the ATDE and the T700-GE-701 is presented in table 11. All performance numbers presented for the ATDE, and used in the Gem 2 analysis, are average values of the demonstrator engines produced by Allison and Lycoming.

Lapse Rates

The temperature lapse rate (KT), and pressure lapse rate (KD), must be determined to use equation (14) (shaft horsepower as a function of flight condition). Engine performance at temperatures and altitudes other than SLS are required to calculate these directly. Typically, the calculation of KT is made using SLS data and the SL/95°F data for each engine rating, whereas the calculation of the KD is made based on SLS and 4000 ft/95°F data (data at higher altitudes would be required to determine pressure lapse rates above 4000 ft). These data were not available for the Gem 2, so values for KT and KD were assumed, based on the average lapse rates of the T700-GE-701 and ATDE engines. Typically, several values of KD are required to model engine performance over a wide altitude range. For this

example we are interested in a small altitude range (0 to 4,000 ft), which can be modeled with a single value of KD .

Additional data in the form of horsepower versus airspeed are required to directly calculate the ram-air effect parameter, N . These data were not readily available for the Gem 2, so ATDE data were used. The ATDE is similar in size and mass flow to the Gem 2. Thus, N (ram-air effect parameter) for the Gem 2 was assumed equal to the ATDE. The parameters used to model the Gem 2 uninstalled engine power available are presented in table 12.

Calculation of Fuel Flow Rates

The publicly available Gem 2 SFC values are not sufficient to model the fuel-flow parameters (see eq. (15)). Additional SFC values at other power settings and atmospheric conditions are necessary. These SFC values were estimated based on available data on the ATDE. Ratios of SFC values for the ATDE were assumed equal to the Gem 2. For example, the ATDE has a SFC for MCP 1% greater than the SFC for IRP. This relationship was assumed for the Gem 2, so the SFC for MCP was 101% of SFC IRP (0.528 lb/hr/shp). This value of SFC combined with the publicly available SFC value at 400 shp (see table 10) was used to calculate the slope of the fuel-flow curve. This slope was assumed valid for IRP also. Similar ATDE SFC ratios were used to estimate Gem 2 fuel flow at 4000 ft/95°F for MCP and IRP. These estimated fuel flows were used to calculate the parameter MF (calibrates the fuel-flow curve intercept to the effect of ambient temperature and pressure).

The ram-air effect parameter (NF) cannot be calculated directly because of the lack of readily available data on airspeed versus SFC for a given engine power setting. This parameter was assumed to be the same as that used for modeling of the ATDE engine. The parameters used to model the Gem 2 fuel flow are presented in table 13.

Engine Installation Effects, Accessory Power, and Transmission Loss

Specific data on engine installation effects were not readily available for the Gem 2 in the A129. The installation losses were estimated based on knowledge of the installation arrangement and by making comparisons with known AH-64 installation data. The Gem 2 has an integral IPS so the uninstalled-power-available data were assumed to include the power loss to run the IPS. The losses associated with the inlet duct and IRS operation were assumed to be a constant percentage of the power required at the engine output shaft. The inlet ram efficiency (η) was assumed to be the same as that used to model the AH-64. The ratio of A129 accessory power required to installed power was assumed to be the same as used to model the AH-64. Equations (16) and (17) were used to estimate the A129 transmission loss. The parameters used to model the A129 engine installation effects, accessory power, and transmission loss are tabulated in table 14.

A129 WEIGHT ESTIMATION

The weight of the A129 was estimated using previously described estimation methods. The primary mission configuration was selected as the baseline for investigation. The A129 was divided into empty

weight and useful load for estimation. The empty weight was decomposed into weight groups at a Mil-Std-1374A, Part I, level of detail. Weight groups were identified as either scaled or fixed to determine how they would be estimated. Previously derived parametric weight equations were used with A129 inputs to estimate scaled weights. Each weight equation was calibrated with the reference helicopter (AH-64 or AH-1) and adjusted for the effect of advanced technology (e.g., use of composite materials). Fixed weights were assumed to be the same as those for the AH-64. They were estimated at a Mil-Std-1374A, Part II, level of detail based on AH-64 components. Scaled and fixed weight estimates were verified and combined to arrive at the A129 empty weight. Useful load weight for this example was determined to be the difference between the published primary mission gross weight and the estimated empty weight. Published weights of items included in useful load are presented in table 15. Weight fractions (based on primary mission gross weight) for A129, AH-1, and AH-64 were calculated and compared.

A129 Weight Groups

The A129 in its primary mission configuration was selected as the baseline for investigation. The primary mission gross weight includes empty weight and mission useful load. The useful load consists of two crewmembers, eight TOW missiles and launching equipment, mission fuel with reserve, and trapped fluids. The empty weight was decomposed into functional groups, and then into weight groups at the level of detail of Mil-Std-1374A, Part I (Group Weight Statement).

A129 Weight Estimates

Weight groups were estimated after being categorized as either scaled or fixed. A129 scaled weights were generally assumed to possess AH-64 levels of military requirements and technology. Exceptions appeared in the function group structure. The wing, tail rotor, vertical tail, and horizontal tail were assumed to be similar to those of the AH-1 based on configurations, dimensions, and functions. Fixed weights, with the exception of the engines, were assumed to be equal to AH-64. The weight of the Rolls-Royce Gem 2 was taken from publicly available literature.

Scaled Weights

A129 scaled weights were estimated using parametric equations. The equations used for A129 weight estimates were generated by this office before the current study. All of the weight equations, except wing, were generated statistically using least-squares linear regression analysis. The wing weight was estimated using a simple nonstatistical parametric equation. The statistical parametric equations met the following criteria:

1. Average absolute error (calculated vs actual weight) less than 10%
2. Ten or more helicopters used (with current helicopters represented)
3. Wide range of input values used (representing current helicopter sizes and types)
4. Statistical criteria (e.g., significance and correlation of variables)

Detailed information regarding multivariate linear regression analyses and statistical criteria appears in other sources (refs. 23 and 24).

Calibration factors were used to allow the parametric weight equations to exactly estimate the reference helicopter scaled weights (table 16). All equations used to estimate scaled weights were calibrated with AH-64 except wing, tail rotor, vertical tail, and horizontal tail, which were calibrated with AH-1. AH-64 or AH-1 input values were used in each weight equation to arrive at an estimated weight. The estimate was then compared with the actual weight. The factor required to adjust the estimate to the reference helicopter's actual weight was determined to be the calibration factor.

Technology factors were used to reflect the effect of optimized composite structures on weight estimates based on "conventional" structures (see table 16). Groups that made extensive use of composite materials were assumed to weigh between 80% and 90% of the group weight when made of conventional metallic materials (based on the results of the Advanced Composite Airframe Program, ACAP, ref. 25). The range represents the percentage if the group was exclusively composite materials (80%) or a mix of composites with metallics (90%). Technology factors for composites use were applied to all of the A129 weight groups in the functional group Structure except Landing Gear.

Fixed Weights

A129 fixed weights were estimated using component and group weights from the reference helicopter assumed to have similar mission requirements. The AH-64 was used as the reference helicopter for estimating A129 fixed weights. All weights of the functional group Equipment, and Cockpit Controls were based on AH-64 components and groups. The actual engine weight for Rolls-Royce Gem 2 was located in publicly available literature and used instead of an estimate.

A129 equipment components were identified from literature whenever possible. Components that were the same or similar were determined using literature sources and an AH-64 actual weight report (ref. 13). AH-64 component weights were used as estimates of A129 fixed weights.

When specific A129 component information was not available, general capabilities in common with AH-64 were identified. The weights of AH-64 components which contributed to the capability were used for A129 estimation. The A129 was known, for example, to possess the capability to detect and extinguish engine fires. The weights of components that contributed to a similar AH-64 capability were used as A129 estimates, though the exact A129 equipment was unknown.

Differences between the A129 and AH-64 were also useful in estimating fixed weights. The AH-64 has a separate auxiliary power unit, whereas the A129 uses the disengaged engines for the same purpose. Both the A129 and the AH-64 have electrical systems, but different systems are powered. The number of A129 electrically powered systems are fewer than for AH-64; therefore, its weight is proportionally less. There are other notable differences that enabled A129 fixed weights to be estimated with greater certainty.

A129 Weight Estimation Verification

The A129 empty weight estimate was compared with the empty weight appearing in publicly available literature. Scaled weights and fixed weights were evaluated against comparable AH-64 and AH-1 weights. Differences were noted and causes for deviations identified.

Gross weight fractions were also used to compare A129 weight estimates with actual AH-64 and AH-1 values. Mission gross weights were the basis for weight fractions. A129 weight fractions, for both scaled and fixed weights, were evaluated against comparable AH-64 or AH-1 fractions in much the same way that the weights were. As before, differences were noted and causes for deviations identified.

A129 ANALYSIS RESULTS

The results of the ARTA analysis were compared with flight-performance data presented in publicly available literature (table 17) (ref. 11). The results estimated by ARTA compare well with the published values. Differences in maximum vertical rate of climb are due to a low ARTA estimate for the helicopter vertical flat-plate drag.

A summary of A129 estimated weights and weight fractions is presented in table 18. The estimated empty weight, 5,676 lb, compares favorably with the published value 5,575 lb (a difference of 101 lb or 1.8%). Estimated A129 scaled and fixed weights and fractions were compared with AH-64 values (table 19). Estimated scaled weight fractions were all within 2% of comparable AH-64 fractions. Fixed-weight fraction deviations were more pronounced, but were attributed primarily to differences in A129 and AH-64 mission requirements.

REFERENCES

1. Johnson, W.: A Comprehensive Analytical Model of Rotorcraft Aerodynamics and Dynamics. Part I. Analysis Development. NASA TM-81182, 1980.
2. Johnson, W.: Development of a Comprehensive Analysis for Rotorcraft. I. Rotor Model and Wake Analysis. Vertica, vol. 5, no. 2, 1981.
3. Johnson, W.: Development of a Comprehensive Analysis for Rotorcraft. II. Aircraft Model, Solution Procedure and Applications. Vertica, vol. 5, no. 3, 1981.
4. Johnson, W.: Helicopter Theory. Princeton University Press, Princeton, NJ, 1980.
5. Dadone, L.; and Fukushima, T.: A Review of the Design Objectives for Advanced Helicopter Rotor Airfoils. Presented at the American Helicopter Society Symposium on Helicopter Aerodynamic Efficiency, Mar. 1975.
6. Gessow, A.; and Crim, A.: A Theoretical Estimate of the Effects of Compressibility on the Performance of a Helicopter Rotor in Various Flight Conditions. NACA TN-3798, 1956.
7. U.S. Department of Defense Dictionary of Military Terms. Greenhill Books, NY, 1987.
8. Weight and Balance Data Reporting Forms for Aircraft (Including Rotorcraft). Military Standard 1374A, U.S. Department of Defense, Washington, D.C., Sept. 1977.
9. Desjardins, S.; Laananen D.; and Singley, G.: Aircraft Crash Survival Design Guide, Vol. I. Design Criteria and Checklists. USARTL-TR-79-22A, Fort Eustis, VA, Dec. 1980.
10. Jane's All the Worlds Aircraft. Jane's Information Group, Inc., Alexandria, VA, 1988.
11. A129 Mangusta Light Multirole Attack Helicopter. Brochure, Agusta Helicopter Division, Milano, Italy, 1989.
12. Lovera, D.: The Agusta A129. Vertiflite, Nov./Dec. 1980.
13. Actual Weight and Balance Report AH-64A Advanced Attack Helicopter. Production Version No. 60, MDHC 77-W-8016-3, McDonnell Douglas Helicopter Company, Dec. 1986.
14. Air Vehicle Technical Description Data for the AH-64A Advanced Attack Helicopter. HHI 77-X-8002-3, Hughes Helicopters, Mar. 1984.
15. Aerodynamic Characteristics of Mi-24D and YAH-64 Attack Helicopters without Rotors. AVRAD-COM TR 82-B-4, U.S. Army Aviation Research and Development Command, St. Louis, MO, May 1982.
16. Airworthiness and Flight Characteristics (A&FC) Test of YAH-64 Advanced Attack Helicopter; Prototype Qualification Test: Government (PQT-G), Part 3; and Production Validation Test: Government (PVT-G) for Handbook Verification. Final Report (U), USAAEFA Project No. 80-17-3, U.S. Army Aviation Research and Development Command, St. Louis, MO, Oct. 1982.

PRECEDING PAGE BLANK NOT FILMED

PAGE 24 INTENTIONALLY BLANK

17. First Article Preproduction Tests of the AH-64A Helicopter. Formal Report (U), USAAEFA Project No. 84-10, U.S. Army Aviation Systems Command, St. Louis, MO, Nov. 1984.
18. Hoerner, Sighard: Fluid Dynamic Drag: Practical Information on Aerodynamic Drag and Hydrodynamic Resistance (U), Dr.-Ing. S.F. Hoerner, Midland Park, NJ, 1965.
19. Rotor & Wing International 1987 Defense Buyer's Directory. PJS Publications, Inc., Peoria, IL, Jan. 1987.
20. T700 Turboshift Engine. Brochure No. AEGB-3/85-5374L, General Electric Company, Lynn, MA, Mar. 1985.
21. Allison Model 280-D1 Advanced Technology Engine. Brochure No. GTP 5054, Allison Gas Turbine Division, General Motors Corp, Indianapolis, IN.
22. Advanced Technology Turboshift Engine. AVCO Lycoming PLT34B-1 Brochure, AVCO Lycoming Division, Stratford, CN.
23. Hamburg, Morris: Statistical Analysis for Decision Makers. 4th ed., Harcourt Brace Jovanovich, NY, 1987.
24. Burford, Roger: Statistics: A Computer Approach. Charles E. Merrill, Columbus, OH, 1968.
25. Post-Design Weight Analysis Report Advanced Composite Airframe Program (ACAP). SER-750045, Sikorsky Aircraft, Stratford, CN, Mar. 1985.

Table 1. AH-64 Flight test conditions.

Figure	Operating gross weight, lb	Density altitude, ft	Equivalent ISA temperature, °F
13	14,560	7,630	ISA + 32.3
14	14,770	10,000	ISA + 32.6
15	14,694	7,120	ISA + 61.4

Table 2. Transmission and accessory losses applied to AH-64 CAMRAD results.

Airspeed, KTAS:	0	20	40	60	80	100	120	140	150	160
Losses, hp:										
Fig. 13	210	205	189	177	175	181	192	205	211	214
Fig. 14	210	206	192	181	177	181	190	205	211	
Fig. 15	210	205	189	176	173	179	190	203	210	214
Fig. 16	210	203	186	176	178	189	203	215	218	

Table 3. A129 MPP model main-rotor empirical parameters.

Parameter	Value
Nonuniform inflow coefficients (see eq. (1))	
CFNUH	1.085
CFNUI	1.085
Rotor ave. profile drag coefficients (see eq. (4))	
CD0	0.008
FK	0.010
Stall coefficients (see eqs. (9) and (10))	
CSTL	0.040
DSTL	0.100
<i>ESTL</i>	1.140
FSTL	1.500
Drag divergence Mach number coefficients (see eq. (11)) for $-0.4 \leq C_l \leq 0.4$	
C ₀	0.750
C ₁	0.000
C ₂	-0.272
C ₃	-0.119
C ₄	0.166
Drag divergence Mach number for $C_l > 0.4$	
Mdd	0.700

Table 4. Input data for main rotor.

Parameter	Value	Source
Diameter, ft	39.04	Jane's All The World's Aircraft
Number of blades, N.D.	4	Jane's All The World's Aircraft
Blade chord, ft	1.29	Measured from figure 8
Solidity, N.D.	0.08414	Calculated from above
Tip speed, ft/sec	707	Advertising literature
RPM	346	Advertising literature
Twist, deg	-9	AH-64 value assumed
Root cut out, % radius	14.9	Measured from figure 8
Blade lift curve slope, /rad	5.73	AH-64 value assumed
Blade angle for zero lift, deg	0.0	AH-64 value assumed
Tip loss factor, N.D.	0.97	AH-64 value assumed
Mast tilt, deg	5.0 (fwd)	AH-64 value assumed
Rotor airfoil data		AH-64 technology assumed

Table 5. Input data for tail rotor.

Parameter	Value	Source
Diameter, ft	7.35	Jane's All The World's Aircraft
Number of blades, N.D.	2	Jane's All The World's Aircraft
Blade chord, ft	0.96	Measured from figure 8
Solidity, N.D.	0.1663	Calculated from above
Tip speed, ft/sec	656	AH-64 ratio
RPM	1704	Calculated from above
Root cut out, % radius	20.4	Measured from figure 8
Blade angle for zero lift, deg	0.0	AH-64 value assumed
Tip loss factor, N.D.	0.97	AH-64 value assumed
Tail rotor blockage ratio, N.D.	0.29	Measured from figure 8
Rotor airfoil data		AH-64 technology assumed

Table 6. Input data for fuselage.

Parameter	Value	Source
Maximum width, ft	3.50	Measured from figure 8
Length (nose to end of tail boom), ft	36.42	Measured from figure 8
Wetted area, ft ²	538	Jane's All The World's Aircraft
Drag coeff. based on wetted area, N.D.	0.0231	AH-64 value assumed
Vertical flight planform area, ft ²	151	Measured from figure 8
Vertical flight drag coeff; N.D.	0.55	AH-64 value assumed
Vert flight flat-plate drag area, ft ²	83.0	Calc. from above
Flat-plate drag W.R.T. pitch angle of attack squared, ft ² /deg ²	0.0305	Scaled AH-64 value
Lift curve slope, ft ² /deg	1.91	Scaled AH-64 value
Zero lift pitch angle, deg	-4.0	AH-64 value assumed
Pitch angle of attack for min drag, deg	-2.0	AH-64 value assumed
Pitching moment constant, ft ³	-26.24	Scaled AH-64 value
Pitching moment slope, ft ³ /deg	5.00	Scaled AH-64 value

Table 7. Input data for wing.

Parameter	Value	Source
Span, ft	11.08	Measured from figure 8
Tip chord, ft	2.50	Measured from figure 8
Theoretical root chord, ft	3.33	Measured from figure 8
Total area, ft ²	32.30	Measured from figure 8
Exposed area, ft ²	20.50	Measured from figure 8
Aspect ratio, N.D.	3.80	Span ² /total area
Zero lift line incidence, deg	0.0	Assumed from drawing
Stall angle, deg	15.0	AH-64 value assumed
2-D lift curve slope, /deg	0.10	AH-64 value assumed
Oswald span efficiency, N.D.	0.27	AH-64 value assumed
Profile drag coefficients constant, N.D.	0.010	Assumed from ref. 18
W.R.T. ZLL angle of attack, /rad	0.0	AH-64 value assumed
W.R.T. ZLL angle of attack squared, /rad ²	-0.93	AH-64 value assumed

Table 8. Input data for empennage

Parameter	Value	Source
Horizontal tail		
Span, ft	9.92	Measured from figure 8
Average chord, ft	1.70	Measured from figure 8
Total area, ft ²	16.90	Measured from figure 8
Aspect ratio, N.D.	5.82	Calculated from above
3-D lift curve slope, /deg	0.06	AH-64 value assumed
Zero lift line incidence, deg	0.0	AH-64 value assumed
Profile drag coefficient, N.D.	0.0160	Assumed from ref. 18
Vertical tail		
Span, ft	6.70	Measured from figure 8
Average chord, ft	3.01	Measured from figure 8
Total area, ft ²	20.20	Measured from figure 8
Aspect ratio, N.D.	2.22	Calculated from above
Zero lift line incidence	0.0	Assumed from figure 8
W.R.T. centerline, deg		
Profile drag coefficient, N.D.	0.0160	Assumed from ref. 18

Table 9. Input data for parasite drag characteristics.^a

Parameter	Value, ft ²	Source
Total aircraft drag (less ordnance)	17.26	Calc using ref. 18
Fuselage	10.02	Calc using ref. 18
Hub	3.90	Calc using ref. 18
Wing	0.33	Calc using ref. 18
Pylons	0.01	Calc using ref. 18
Landing gear	2.45	Calc using ref. 18
Tail rotor hub	0.28	Calc using ref. 18
Horizontal tail	0.27	Calc using ref. 18
Ordnance (8 TOW missiles, no pylons)	3.55	Calc using ref. 18

^aThe following values are for the fuselage reference line at 0° angle of attack.

Table 10. Publicly available Gem 2 engine power and SFC data.^a

Parameter	Value
Intermediate rated power (30 min), shp	881
Maximum continuous power, shp	825
Specific fuel consumption (at max IRP, 881 shp), lb/hr/shp	0.523
Specific fuel consumption (at cruise, 400 shp), lb/hr/shp	0.660

^aSea level standard, static conditions (refs. 10, 19).

Table 11. Gem 2, ATDE, and T700-GE-701 comparison.^a

Parameter	Gem 2	ATDE	T700-GE-701
Intermediate rated power (30 min), shp	881	840	1698
Specific fuel consumption, lb/hr/shp	0.523	0.477	0.462
Compressor pressure ratio	12:1	14:1	15:1
Power turbine speed, rpm	27,000	27,750	20,900
Year first tested	1976	1984	1973

^aSea level standard, static conditions (refs. 10, 19-22). The data presented represent average values for the Allison and Lycoming engines.

Table 12. Gem 2 uninstalled power available parameters.^a

Parameter	Value	Source
Intermediate rated power (IRP)		
KT	1.880	T700-GE-701 and ATDE average
KD (0-4000 ft altitude)	1.063	T700-GE-701 and ATDE average
N	0.85	ATDE value
Maximum continuous power (MCP)		
KT	2.512	T700-GE-701 and ATDE average
KD (0-4000 ft altitude)	1.033	T700-GE-701 and ATDE average
N	0.85	ATDE value

^aSee equation (14).

Table 13. Gem 2 fuel flow parameters.^a

Parameter	Value	Source
Intermediate rated power		
K1, lb/hr/shp	0.119	Gem 2 and ATDE data
K2, lb/hr/shp	0.404	Gem 2 and ATDE data
<i>MF</i>	1.196	Gem 2 and ATDE data
<i>NF</i>	0.30	ATDE value
Maximum continuous power		
K1, lb/hr/shp	0.124	Gem 2 and ATDE data
K2, lb/hr/shp	0.404	Gem 2 and ATDE data
<i>MF</i>	1.334	Gem 2 and ATDE data
<i>NF</i>	0.30	ATDE value

^aSee equation (15).

Table 14. A129 parameters for modeling engine installation effects, accessory power, and transmission loss

Parameter	Value	Source
Inlet loss	0.011	AH-64 value assumed
Inlet ram efficiency	0.85	AH-64 value assumed
Infrared suppressor loss	0.02	AH-64 value assumed
Accessory power loss	0.027	AH-64 value assumed
Transmission rating, shp	1300	Jane's All The World's Aircraft
Gearbox loss at 100% of transmission rated power, %	3.8	AH-64 value assumed

Table 15. Agusta A129 Mangusta useful load weight summary.

Group	Weight, lb	Fraction, %
Gross weight	8157.0	100.0
Useful load	2481.3 ^a	30.4
Crew (2, AH-64)	470.0	5.7
Fuel (usable, fallout)	1178.6	14.5
Fuel (unusable, AH-64: 0.5% max internal fuel weight)	7.5	0.1
Oil (AH-64 & AH-1)	30.0	0.4
TOW missiles (8, A129 marketing literature)	370.4	4.5
TOW tubes (8, AH-1)	104.0	1.3
TOW launchers (4, AH-1)	240.0	2.9
Stores pylons (2, AH-1)	80.8	1.0

^aUseful load weight resulted from subtracting the A129 weight estimate from the published mission gross weight (ref. 10). Publicly available useful load item weights were subtracted until the weight of fuel "fell out."

Table 16. Factors used for A129 empty weight estimation.

Group	Category ^a	Calibration	Technology
Structure			
Wing	Scaled	1.81	0.80
Main rotor	Scaled	0.97	0.85
Tail rotor	Scaled	0.90	0.80
Vertical tail	Scaled	1.03	0.80
Horizontal tail	Scaled	1.02	0.80
Body	Scaled	1.00	0.90
Landing gear	Scaled	1.01	1.00
Nacelles/cowls/air induction	Scaled	0.83	0.80
Propulsion			
Engines	Fixed	—	1.00
Subsystems	Scaled	0.84	1.00
Fuel tanks	Scaled	0.89	1.00
Fuel plumbing	Scaled	0.93	1.00
Gearboxes/rotor shaft	Scaled	0.91	1.00
Intermediate drive shafts	Scaled	1.10	1.00
Flight controls			
Cockpit controls	Fixed	—	1.00
Boosted rotor flight controls	Scaled	1.01	1.00
Non-boosted rotor flight controls	Scaled	0.88	1.00
Flight control hydraulics	Scaled	1.02	1.00
Equipment			
Auxiliary power	Fixed	—	1.00
Utility hydraulics/pneumatic	Fixed	—	1.00
Electrical	Fixed	—	1.00
Instruments/avionics	Fixed	—	1.00
Armament/armor	Fixed	—	1.00
Furnishings/equipment	Fixed	—	1.00
Air conditioning/anti-icing	Fixed	—	1.00
Load/handling	Fixed	—	1.00

^aAll scaled weights were calibrated against AH-64 except wing, tail rotor, vertical tail, and horizontal tail, which were calibrated against AH-1.

Table 17. A129 analysis results.^a

	4000 ft/ISA		4000 ft/90°F	
	Published values	ARTA results	Published values	ARTA results
Max speed at MCP, KTAS	143	142	140	144
Max rate of climb at IRP, ft/min	2300	2260	2300	2270
Max vertical ROC at IRP, ft/min	1020	1400	960	1230

^aConfiguration: eight T.O.W. missiles, PMGW = 8,157 lb.

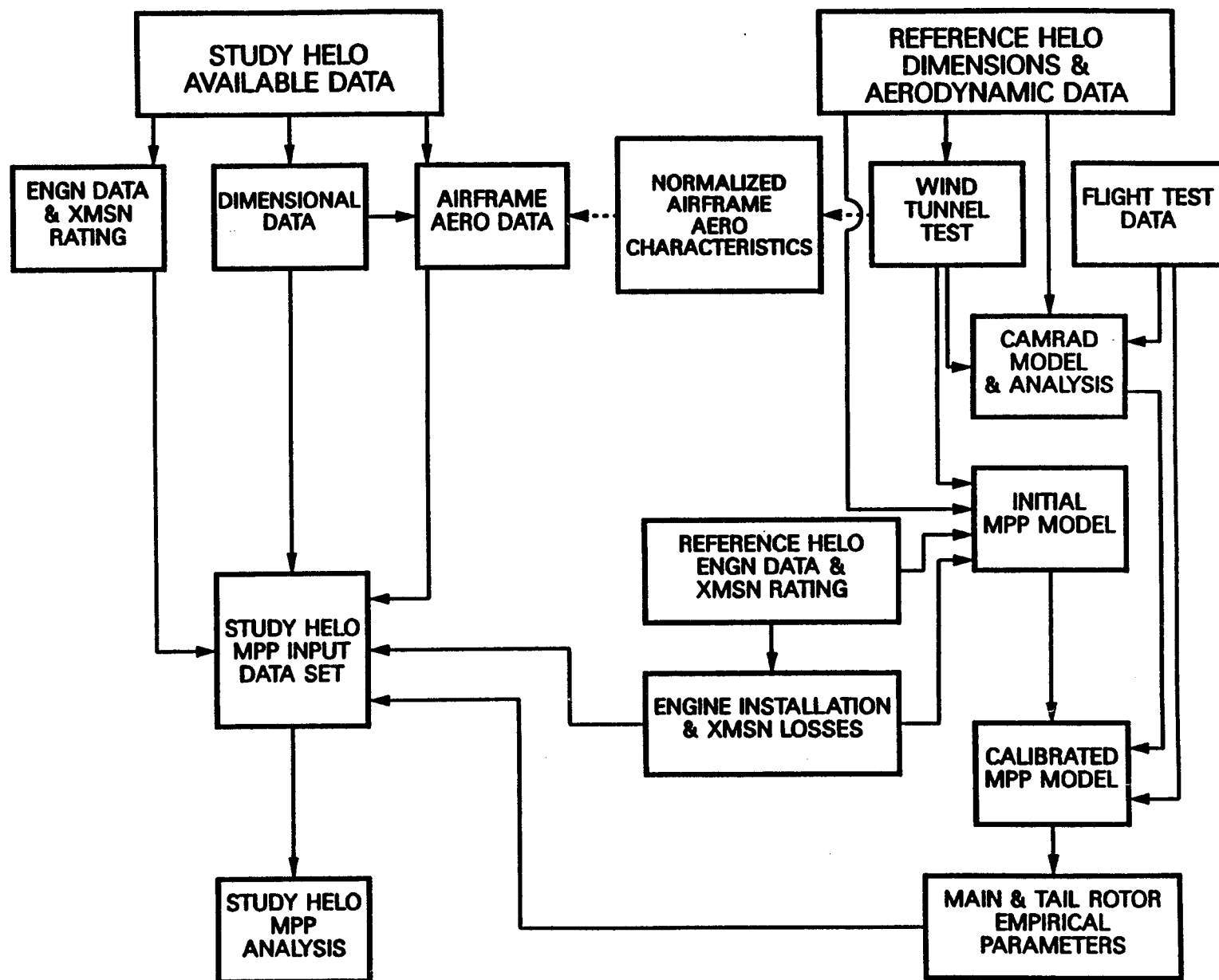
Table 18. Agusta A129 Mangusta weight estimation summary.

Group	Category ^a	Weight, lb	Fraction, %
Gross weight		8157.0	100.0
Useful load		2481.3	30.4
Empty weight		5675.7	69.6
Structure		1914.6	23.5
Wing	Scaled	59.5	0.8
Main rotor	Scaled	573.8	7.0
Tail rotor	Scaled	20.8	0.3
Vertical tail	Scaled	35.3	0.4
Horizontal tail	Scaled	25.7	0.3
Body	Scaled	767.2	9.4
Landing gear	Scaled	315.9	3.9
Nacelles/cowls/air induction	Scaled	116.4	1.4
Propulsion		1741.1	21.3
Engines	Fixed	746.0	9.1
Subsystems	Scaled	137.1	1.7
Fuel tanks	Scaled	189.4	2.3
Fuel plumbing	Scaled	74.3	0.9
Gearboxes and rotor shaft	Scaled	539.8	6.6
Intermediate drive shafts	Scaled	54.5	0.7
Flight controls		360.2	4.4
Cockpit controls	Fixed	44.9	0.6
Boosted rotor flight controls	Scaled	101.1	1.2
Non-boosted rotor flight controls	Scaled	83.2	1.0
Flight control hydraulics	Scaled	131.0	1.6
Equipment		1659.8	20.4
Auxiliary power	Fixed	0.0	0.0
Utility hydraulics/pneumatic	Fixed	0.0	0.0
Electrical	Fixed	234.9	2.9
Instruments/avionics	Fixed	501.4	6.1
Armament/armor	Fixed	544.1	6.8
Furnishings/equipment	Fixed	211.6	2.6
Air conditioning/anti-icing	Fixed	165.1	2.0
Load/handling	Fixed	2.7	0.0

^aAll scaled weights were calibrated against AH-64 except wing, tail rotor, vertical tail, and horizontal tail which were calibrated against AH-1.

Table 19. Comparison of A129 weight estimates with AH-64.

Group	A129		AH-64	
	Weight, lb	Fraction, %	Weight, lb	Fraction, %
Gross weight	8157.0	100.0	14597.5	100.0
Useful load	2481.3	30.4	3683.2	25.3
Empty weight	5675.7	69.6	10914.3	74.7
Structure	1914.6	23.5	3875.6	26.5
Wing	59.5	0.8	166.1	1.1
Main rotor	573.8	7.0	1214.5	8.3
Tail rotor	20.8	0.3	94.5	0.6
Vertical tail	35.3	0.4	124.5	0.9
Horizontal tail	25.7	0.3	108.1	0.7
Body	767.2	9.4	1421.9	9.7
Landing gear	315.9	3.9	518.6	3.6
Nacelles/cowls/air induction	116.4	1.4	227.4	1.6
Propulsion	1741.1	21.3	2789.8	19.1
Engines	746.0	9.1	993.6	6.8
Subsystems	137.1	1.7	121.1	0.8
Fuel tanks	189.4	2.3	283.6	1.9
Fuel plumbing	74.3	0.9	106.2	0.7
Gearboxes and rotor shaft	539.8	6.6	1190.2	8.2
Intermediate drive shafts	54.5	0.7	95.1	0.7
Flight controls	360.2	4.4	907.0	6.2
Cockpit controls	44.9	0.6	119.1	0.8
Boosted rotor flight controls	101.1	1.2	195.6	1.3
Non-boosted rotor flight controls	83.2	1.0	290.0	2.0
Flight control hydraulics	131.0	1.6	302.3	2.1
Equipment	1659.8	20.4	3341.9	22.9
Auxiliary power	0.0	0.0	136.3	1.0
Utility hydraulics and pneumatic	0.0	0.0	61.7	0.4
Electrical	234.9	2.9	405.6	2.8
Instruments and avionics	501.4	6.1	608.6	4.2
Armament and armor	544.1	6.8	1724.7	11.8
Furnishings and equipment	211.6	2.6	211.6	1.4
Air conditioning and anti-icing	165.1	2.0	165.1	1.1
Load and handling	2.7	0.0	28.3	0.2



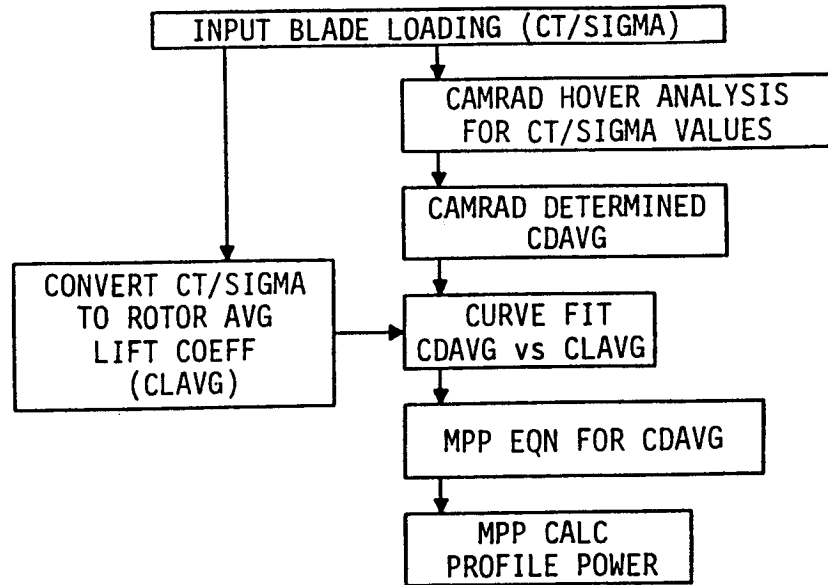


Figure 2. Methodology used to determine MPP main rotor CDAVG.

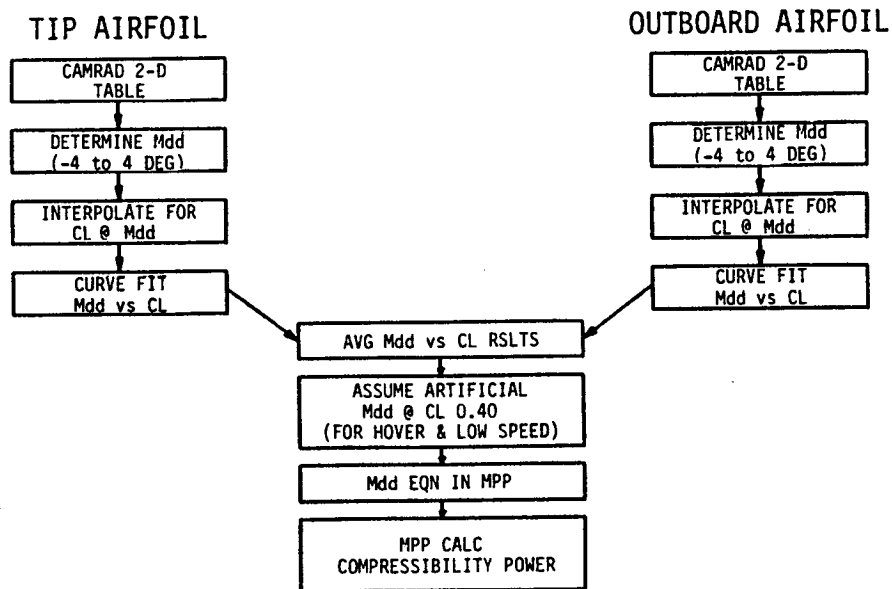


Figure 3. Methodology used to determine MPP main rotor drag divergence Mach number.

STATIC, UNINSTALLED ENGINE POWER AVAILABLE							RAM AIR EFFECTS			
TOTAL, UNINSTALLED ENGINE POWER AVAILABLE										
TOTAL, INSTALLED ENGINE POWER AVAILABLE AT ENGINE OUTPUT SHAFT							LOSSES			
							INLET	EXHAUST		
POWER REQUIRED AT ENGINE OUTPUT SHAFT										
MAIN ROTOR					TAIL ROTOR		X M S N	A C C		
INDUCED		PROFILE		PARASITE	INDUCED				PROFILE	
UNIFORM	NON-UNIFORM	IDEAL	NON-IDEAL							

Blocks are NOT to scale

XMSN = TRANSMISSION
ACC = ACCESSORIES

- IDEAL ROTOR PROFILE POWER INCLUDES THE EFFECTS OF DRAG CREEP DUE TO BLADE LOADING
- NONIDEAL ROTOR PROFILE POWER INCLUDES THE EFFECTS OF DRAG RISE DUE TO STALL AND COMPRESSIBILITY
- PARASITE POWER INCLUDES EFFECTS OF CLIMB OR DESCENT
- POWER REQUIRED MUST BE LESS THAN OR EQUAL TO POWER AVAILABLE FOR STEADY STATE FLIGHT

Figure 4. Breakdown of power available and power required.

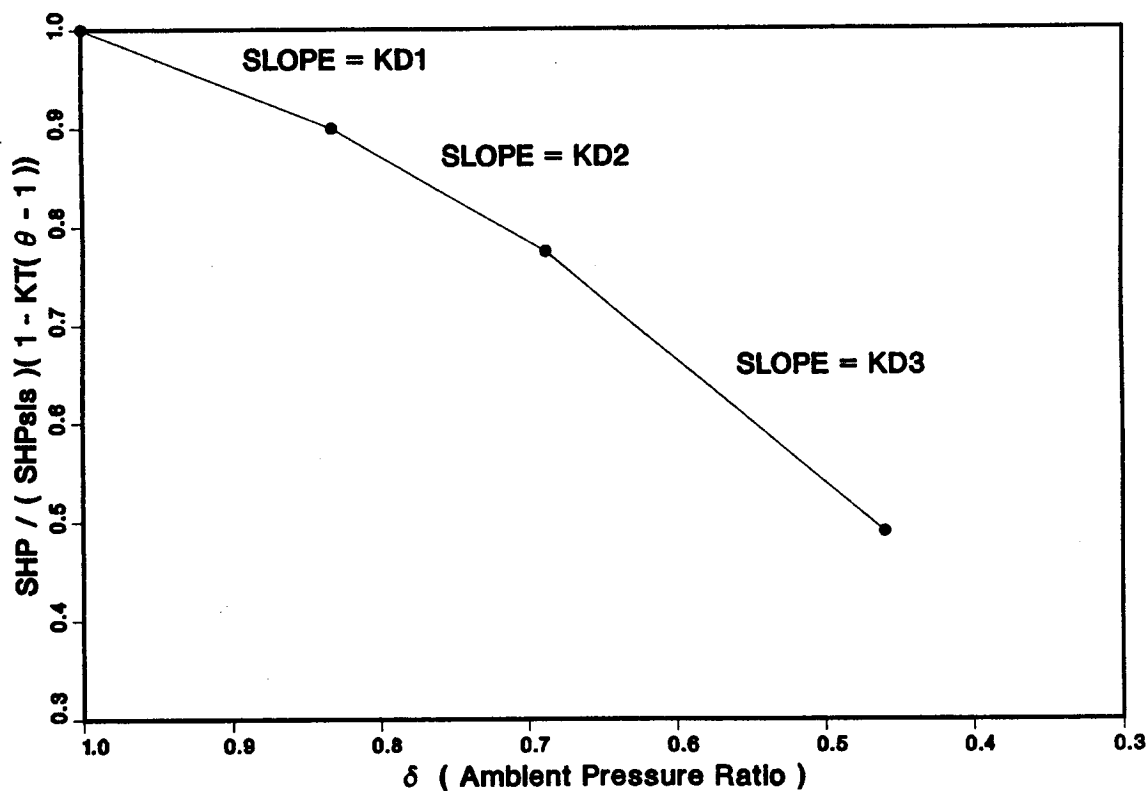


Figure 5. Pressure lapse rate versus ambient pressure ratio.

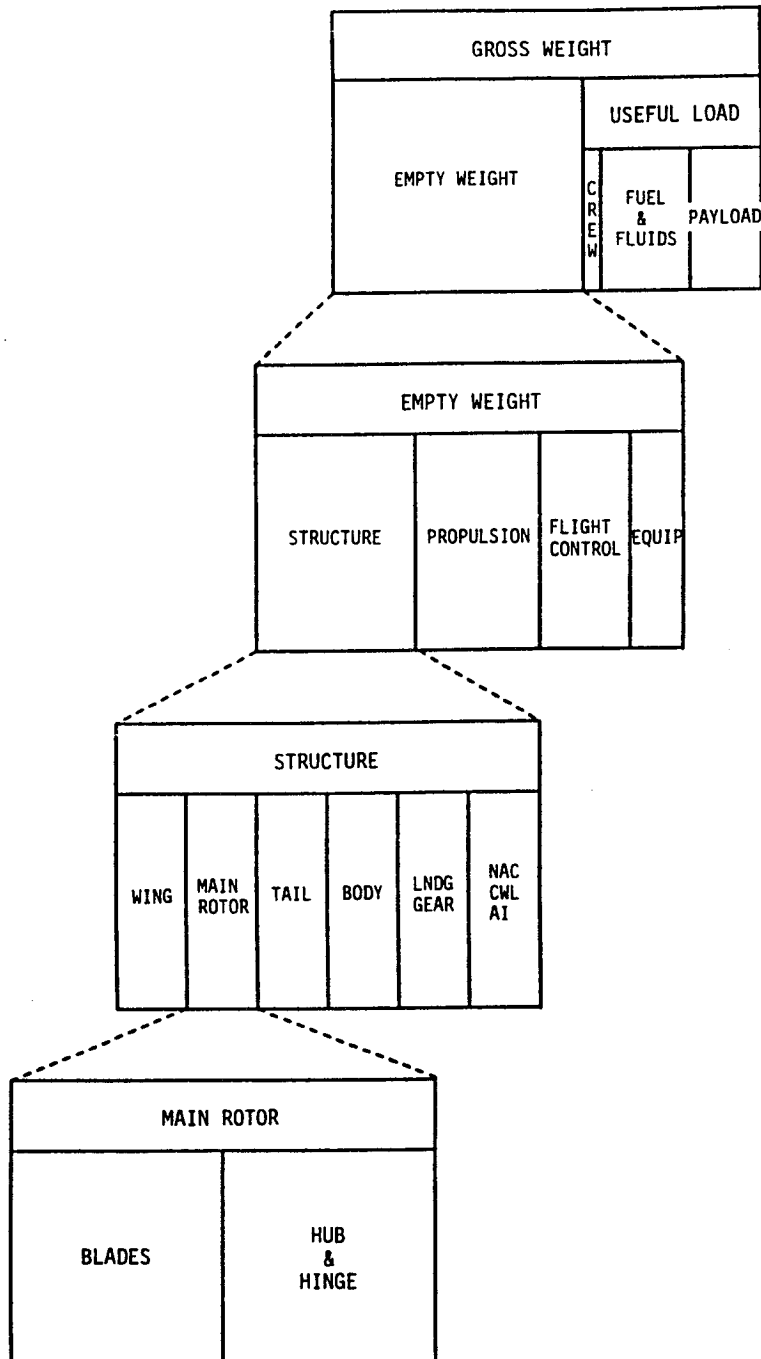


Figure 6. Decomposition of gross weight.

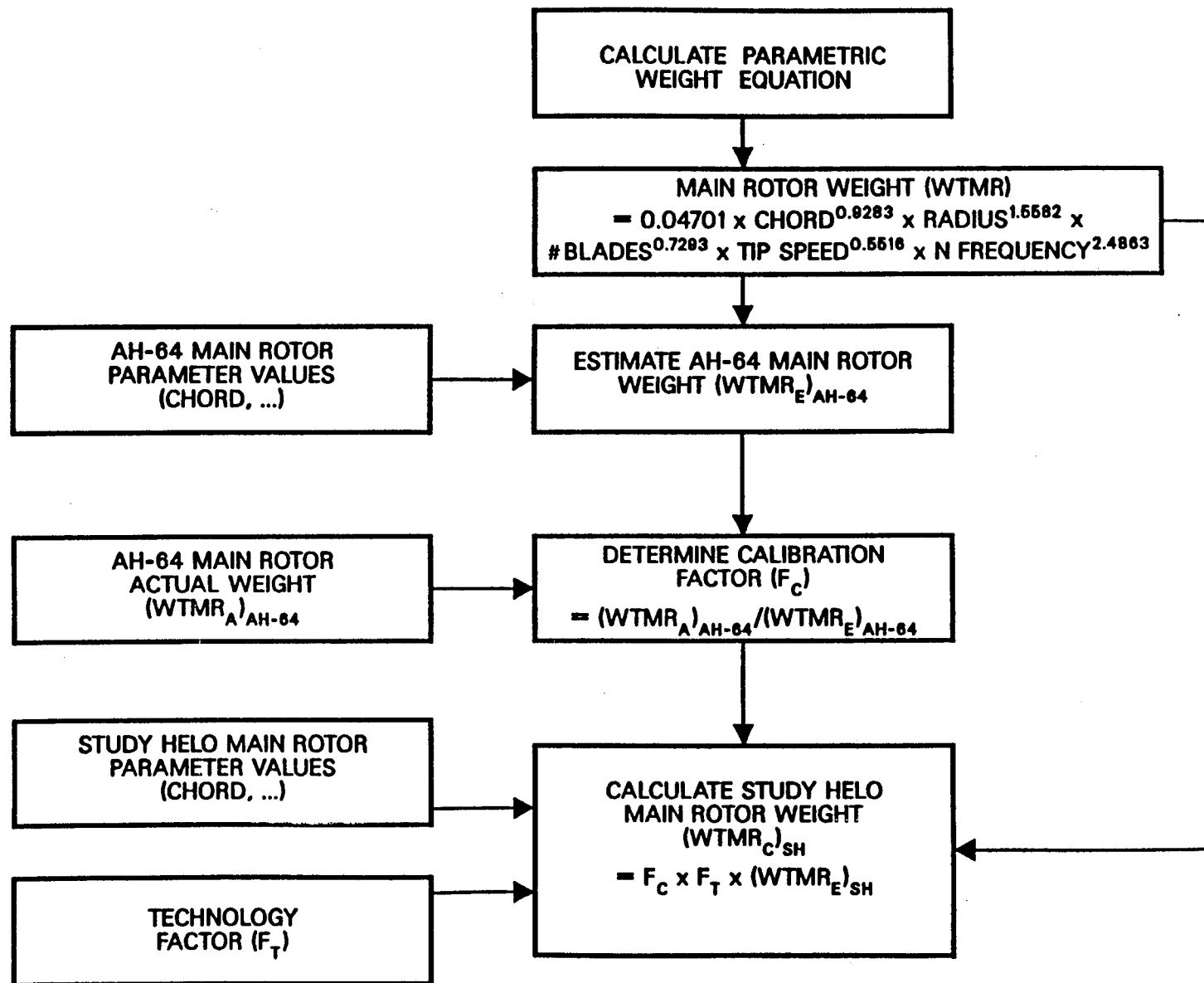


Figure 7. Main rotor scaled weight calculation example.

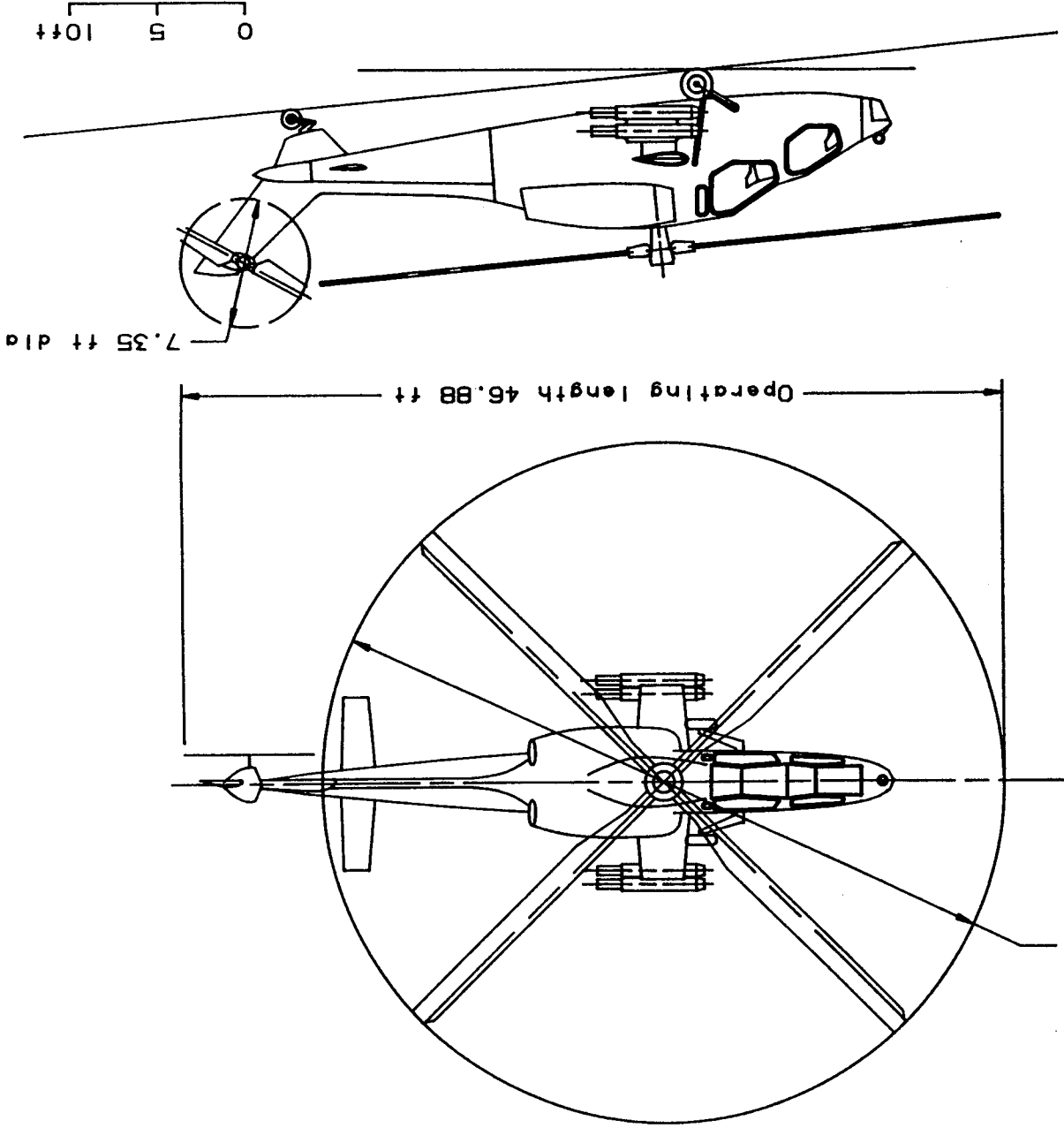
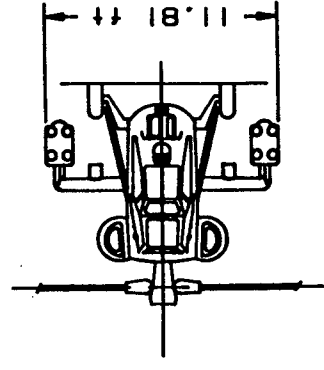
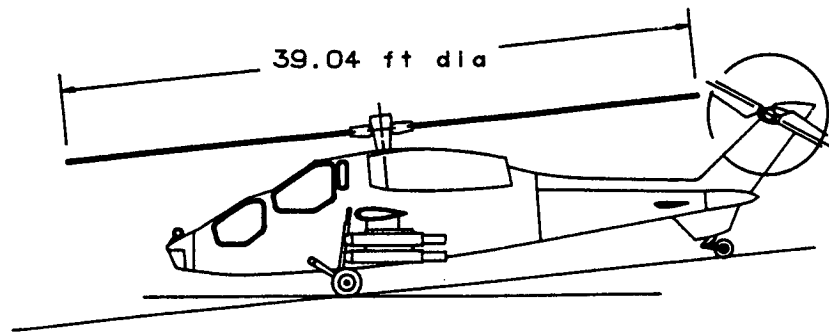
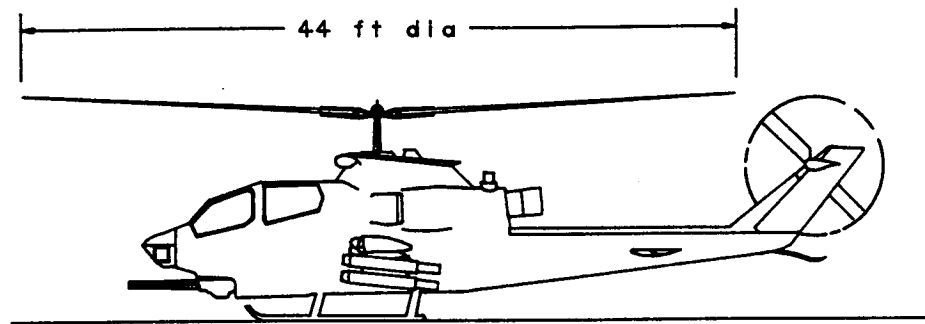


Figure 8. Agusta A129 Mangusta.

A129



AH-1



AH-64

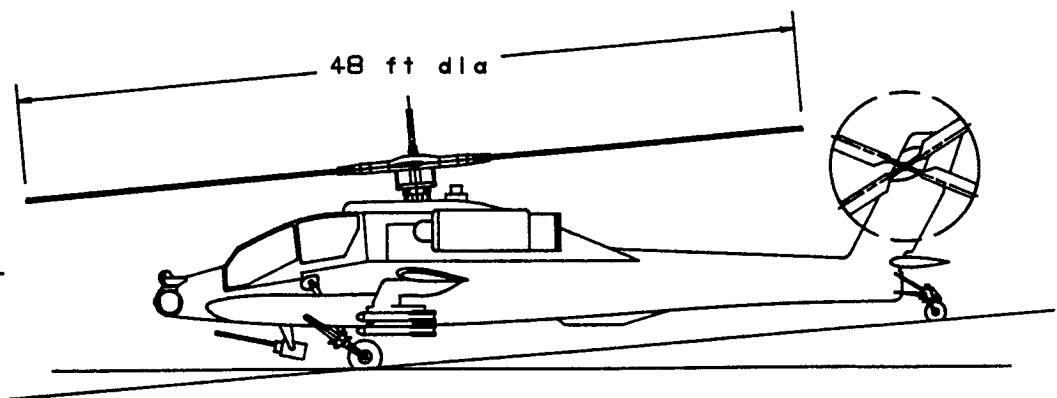


Figure 9. A129, AH-1, and AH-64 size comparison.

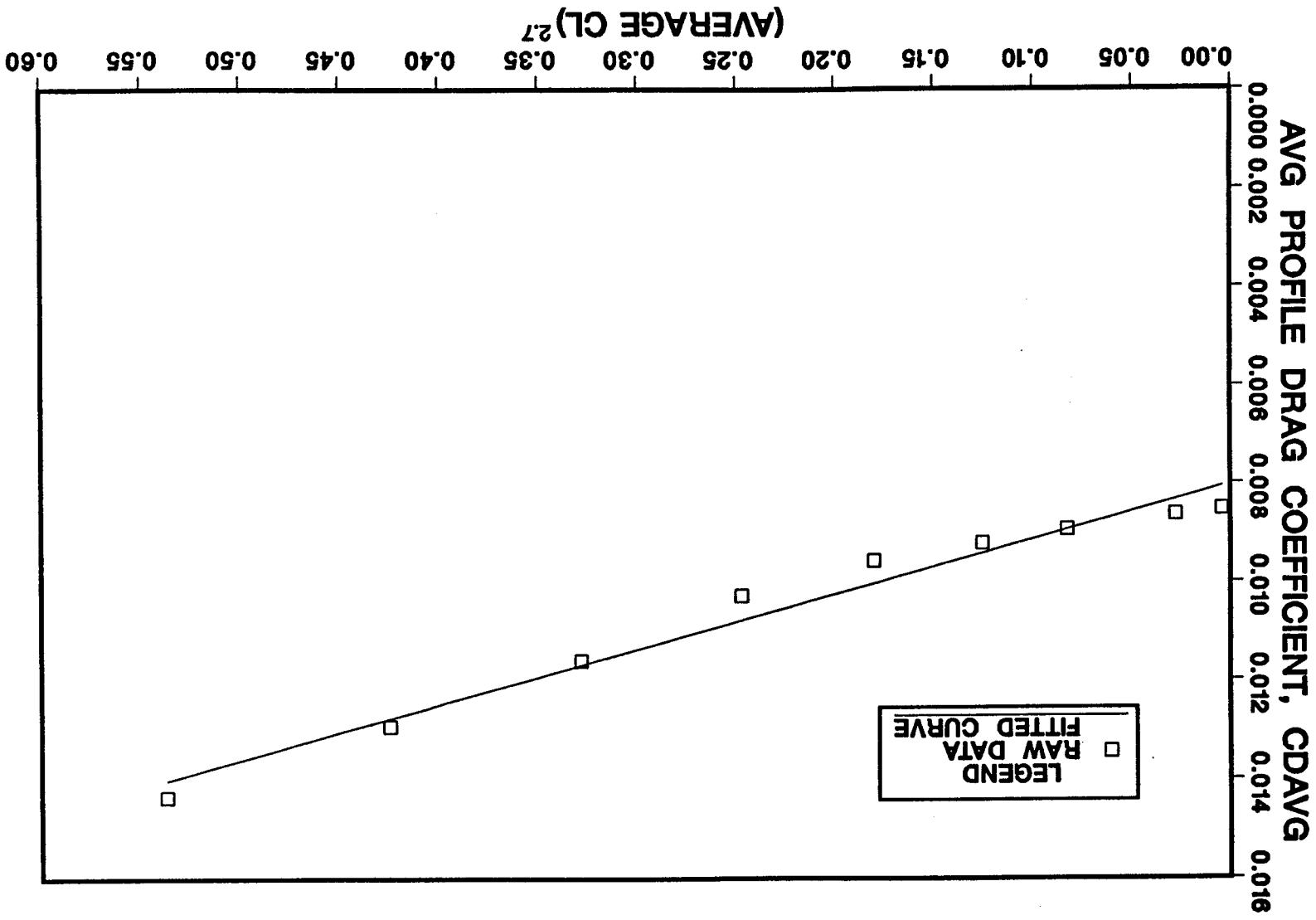


Figure 10. AH-64 average profile drag coefficient, hover, SLS, CAMRAD wind tunnel trim.

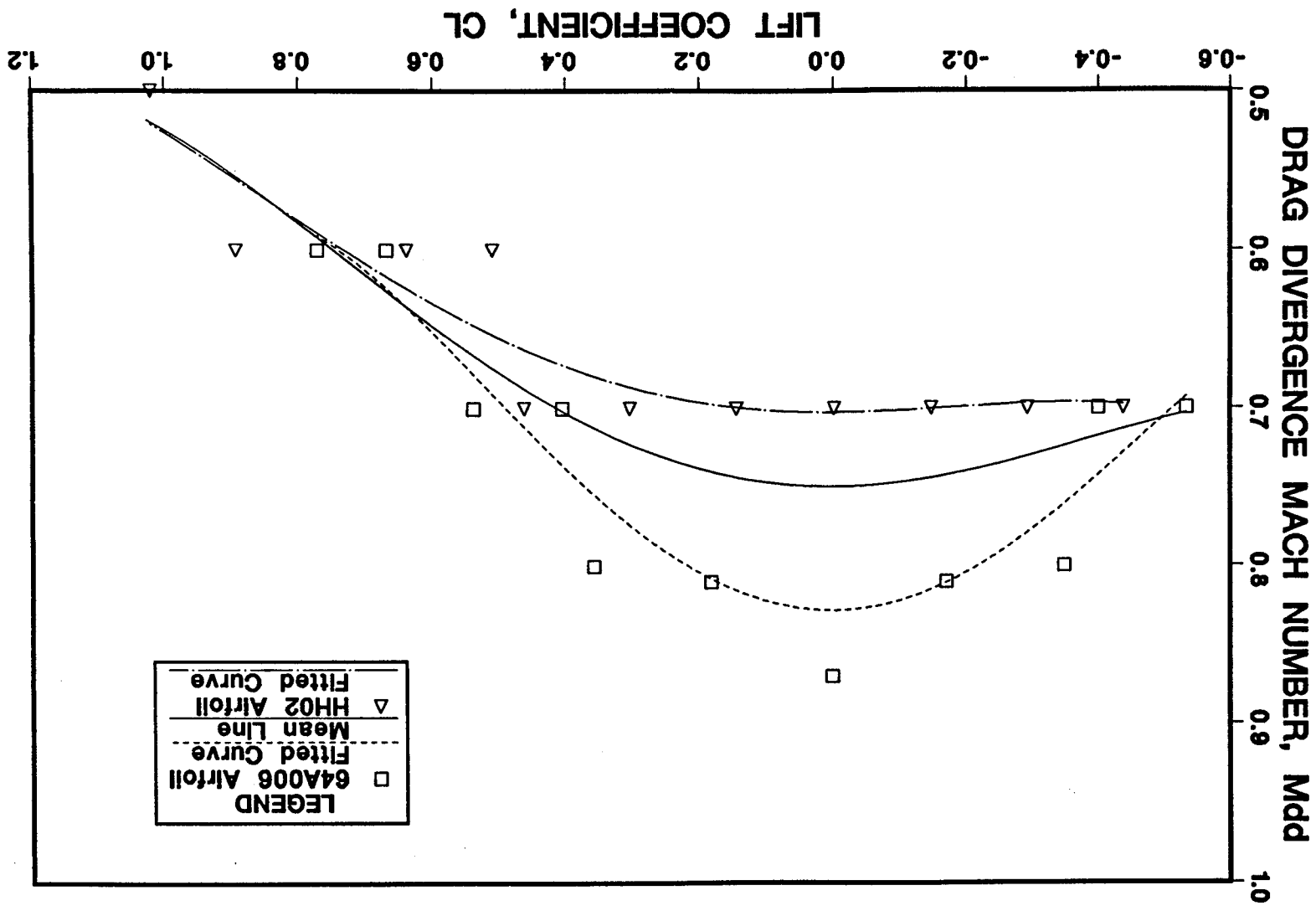


Figure 11. AH-64 drag divergence Mach number versus CL.

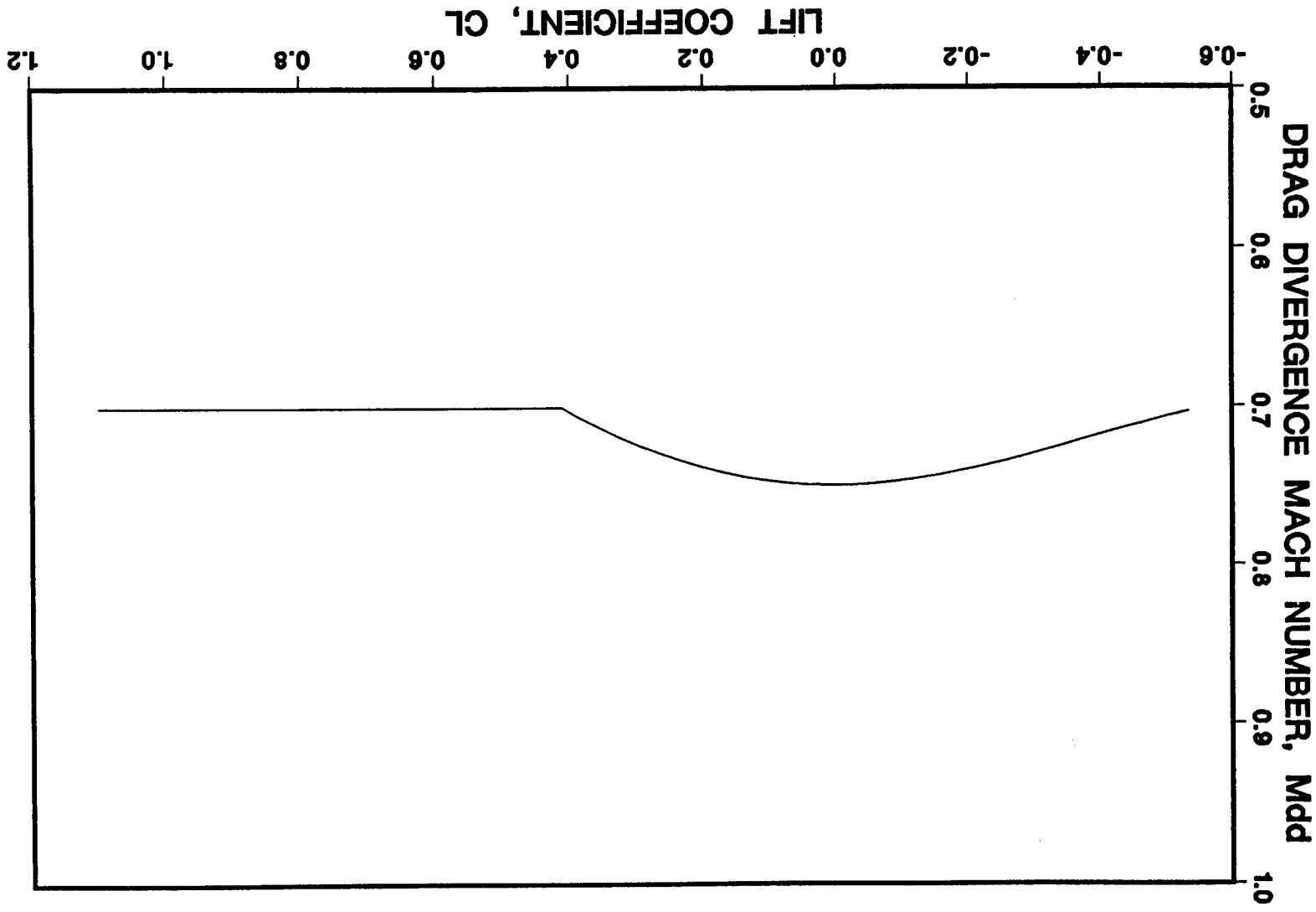


Figure 12. AH-64 drag divergence Mach number versus CL , modified for $CL > 0.40$.

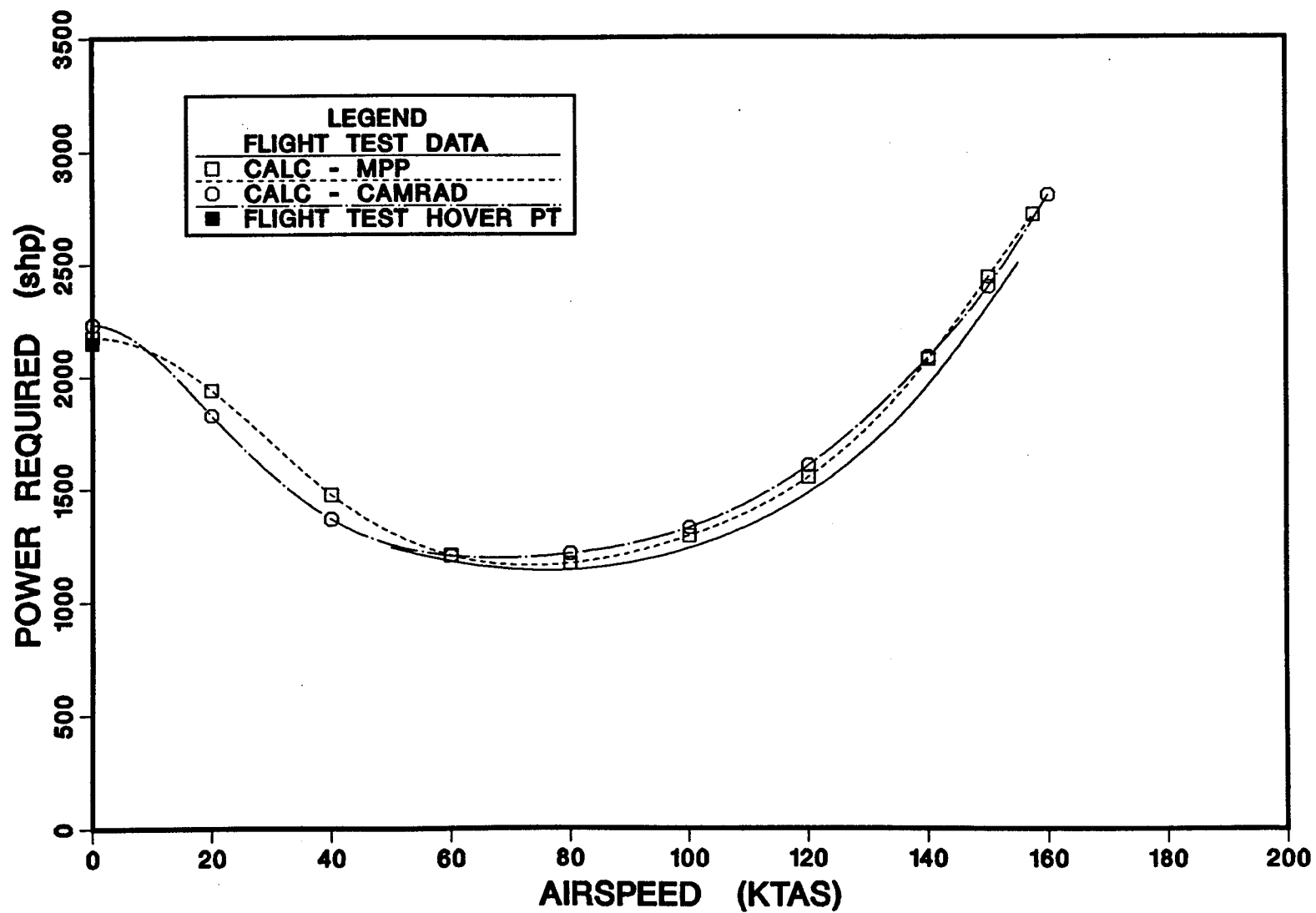


Figure 13. AH-64 level flight power required, GW = 14,560 lb, 8 Hellfire, density altitude 7,630 ft, 65°F.

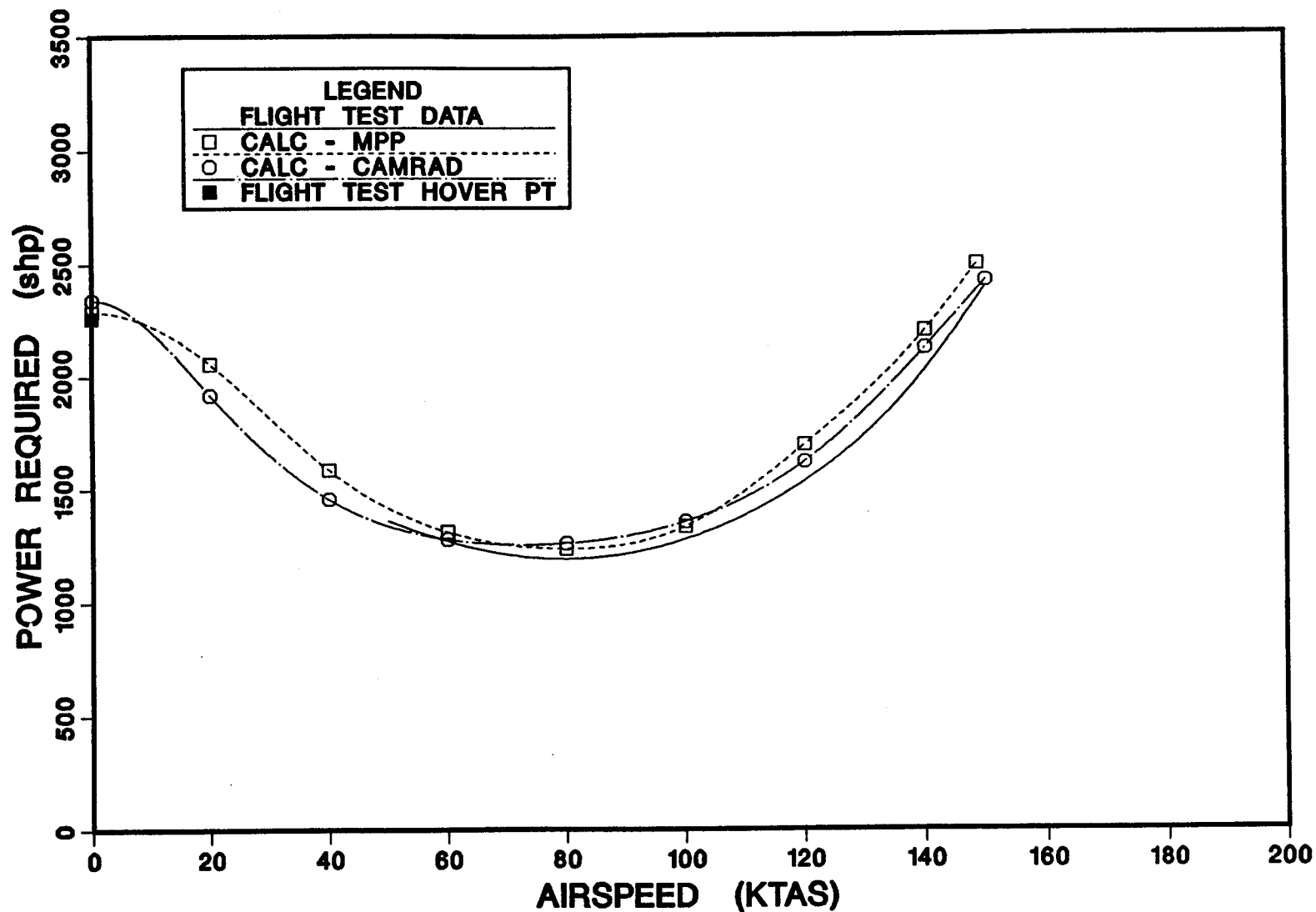


Figure 14. AH-64 level flight power required, GW = 14,770 lb, 8 Hellfire, density altitude 10,000 ft, 56°F.

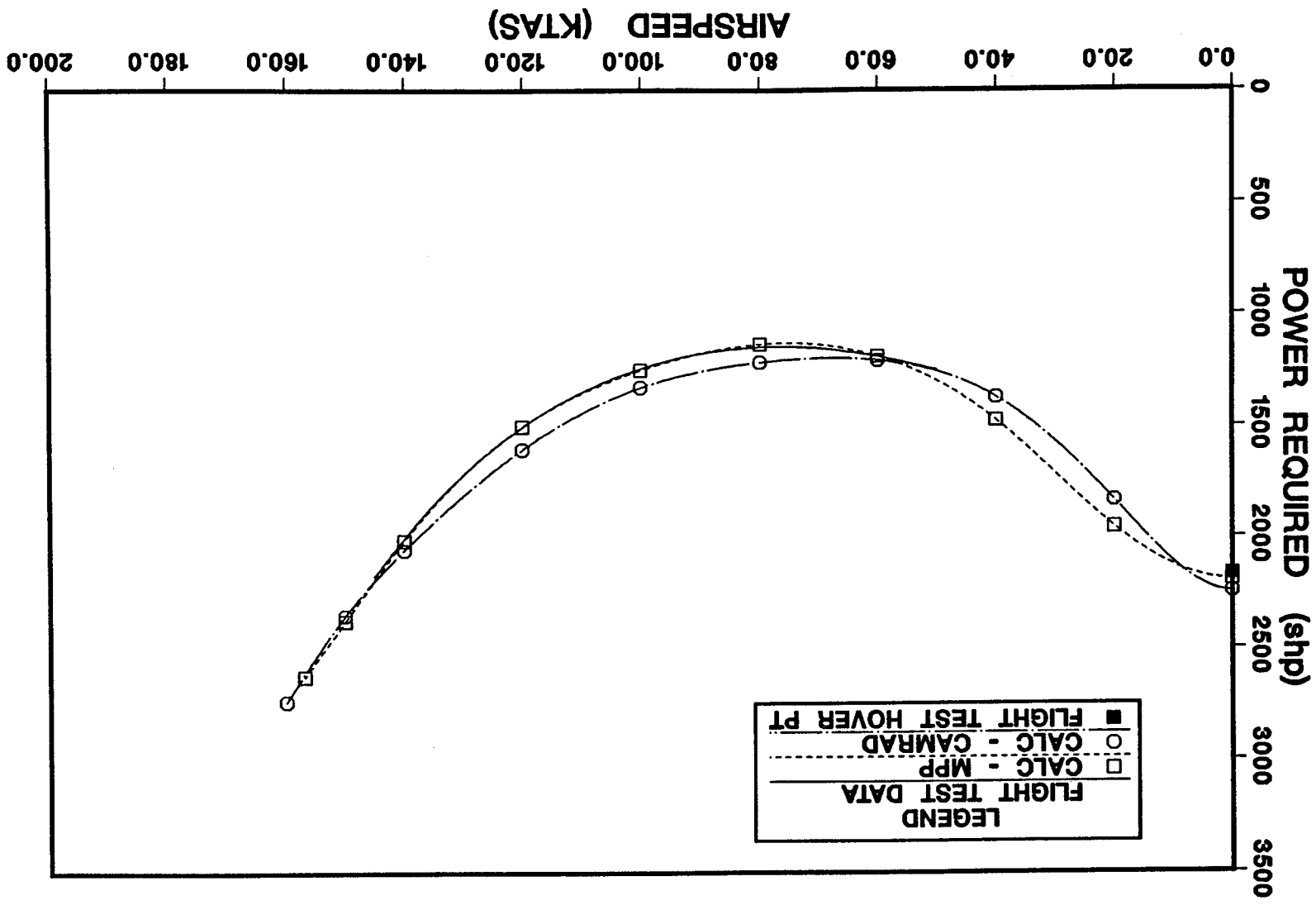


Figure 15. AH-64 level flight power required, GW = 14,694 lb, 8 Hellfire, density altitude 7,120 ft, 95°F.

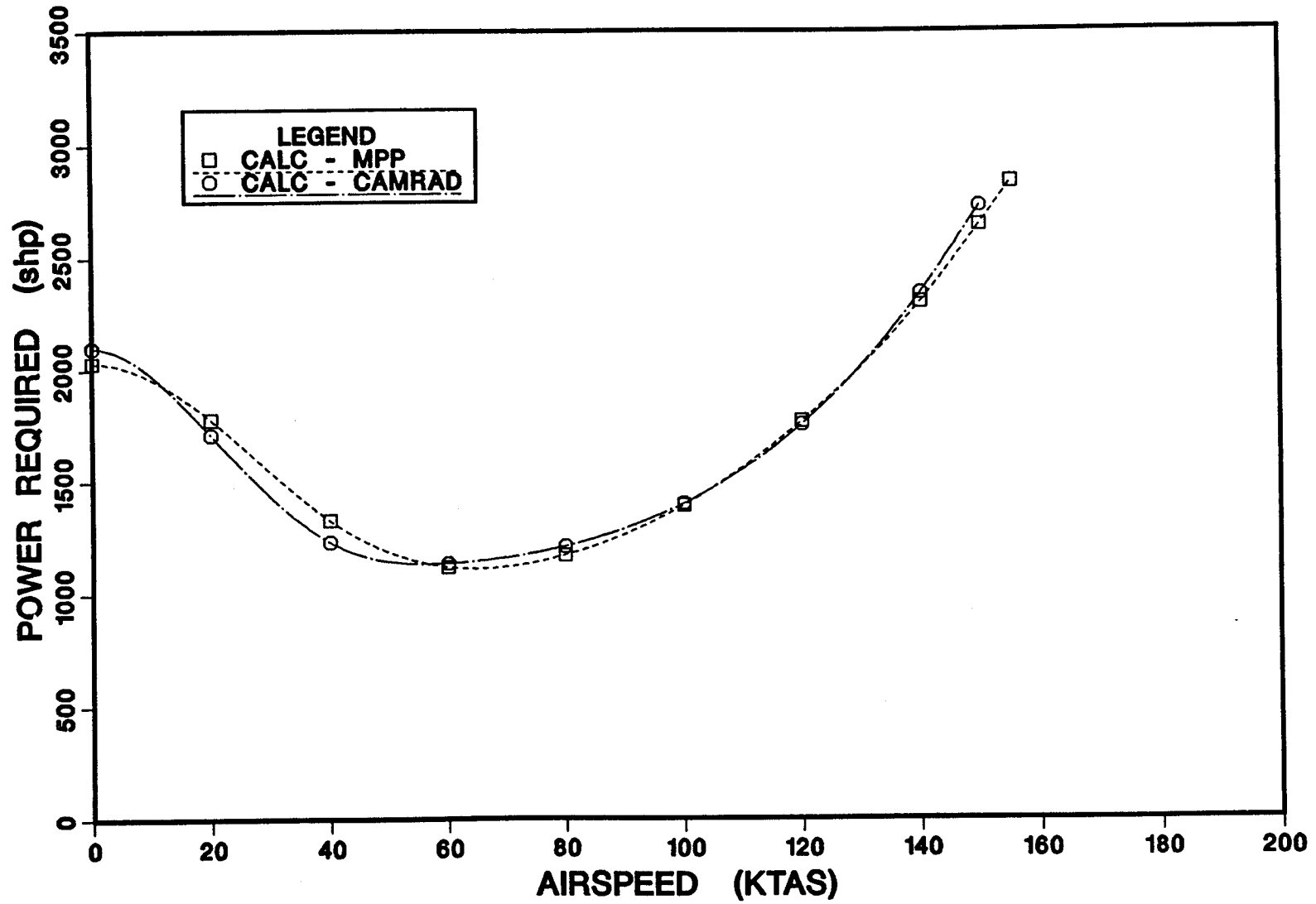


Figure 16. AH-64 level flight power required, GW = 14,660 lb, 8 Hellfire, SLS.

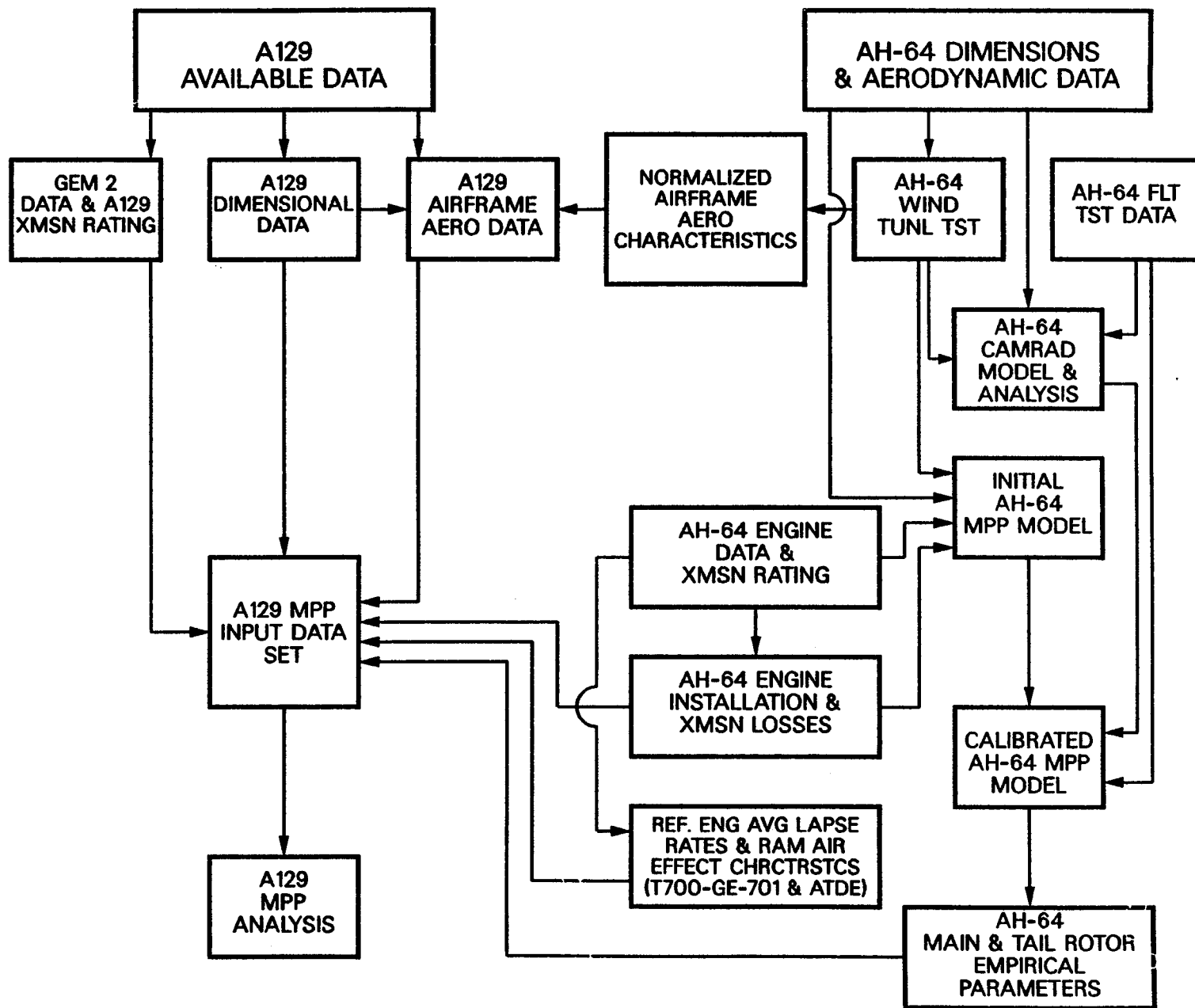


Figure 17. Flowchart of A129 analysis based on AH-64 level of main rotor and airframe aerodynamic technology.

Report Documentation Page

1. Report No. NASA TM-102824 AVSCOM TM-90-F-001		2. Government Accession No.		3. Recipient's Catalog No.	
4. Title and Subtitle Methodology for Estimating Helicopter Performance and Weights Using Limited Data				5. Report Date April 1991	
				6. Performing Organization Code	
7. Author(s) Claudio Baserga, Charles Ingalls, Henry Lee, and Richard Peyran				8. Performing Organization Report No. A-90157	
				10. Work Unit No.	
9. Performing Organization Name and Address Ames Research Center, Moffett Field, CA 94035-1000 and Aeroflightdynamics Directorate, U.S. Army Aviation Research and Technology Activity, Ames Research Center, Moffett Field, CA 94035-1099				11. Contract or Grant No.	
				13. Type of Report and Period Covered Technical Memorandum	
12. Sponsoring Agency Name and Address National Aeronautics and Space Administration, Washington, DC 20546-0001 and U.S. Army Aviation Systems Command, St. Louis, MO 63120-1798				14. Sponsoring Agency Code	
15. Supplementary Notes Point of Contact: Claudio Baserga, Ames Research Center, MS 219-3, Moffett Field, CA 94035-1000 (415) 604-5527 or FTS 464-5527					
16. Abstract A method is developed and described for estimating the flight performance and weights of a helicopter for which limited data are available. The method is based on assumptions that couple knowledge of the technology of the helicopter under study with detailed data from well-documented helicopters judged to be of similar technology. The approach, analysis assumptions, technology modeling, and the use of reference helicopter data are discussed. Application of the method is illustrated with an investigation of the Agusta A129 Mangusta helicopter.					
17. Key Words (Suggested by Author(s)) Helicopter analysis Performance estimation Weight estimation				18. Distribution Statement Unclassified-Unlimited Subject Category - 05	
19. Security Classif. (of this report) Unclassified		20. Security Classif. (of this page) Unclassified		21. No. of Pages 58	
				22. Price A04	